Sensitivity and specificity of the uniform field ERG in glaucoma detection

Asma Hermas

This thesis is submitted to the Faculty of Graduate and Postdoctoral Studies as partial fulfillment of the M.Sc. program in Cellular and Molecular Medicine

Department of Cellular and Molecular Medicine

Faculty of Medicine

University of Ottawa

Abstract

Glaucoma is a silent disease, and by the time patients are diagnosed, there is a significant vision loss, and the clinicians are left to deal with monitoring the disease progression. Therefore, early glaucoma detection would be the ultimate goal for researchers as well as clinicians. This study assessed the sensitivity and specificity of pattern electroretinography (PERG) and uniform field electroretinography (UF-ERG) in detecting glaucomatous changes using the Diagnosys D-341 Attaché-Envoy Electrophysiology System. One hundred eyes of 50 glaucoma patients, including 42 glaucoma-suspect eyes, and 58 confirmed glaucoma eyes went through ophthalmic examination including PERG, UF-ERG (to measure the photopic negative response (PhNR)), Optical coherence tomography (OCT), and standard automated perimetry (SAP). The results were compared to 72 eyes of 36 healthy control subjects. PERG and PhNR parameters showed a significant decrease in the amplitude and longer latency in glaucoma suspects and glaucoma groups compared to the control group. The PhNR amplitude was more sensitive at detecting glaucomatous changes in the glaucoma suspect group than the PERG in terms of low amplitude. Furthermore, two different PERG tests showed a similar ability to recognize individuals without glaucomatous changes and PhNR amplitude and latency were able to identify people with and without glaucoma-related changes, respectively.

Table of Contents

List of tables

List of figures

List of abbreviations

ANOVA	Analysis of variance
ERG	Electroretinography
GCL	Ganglion cell layer
INL	Inner nuclear layer
IOP	Intraocular pressure
IPL	Inner plexiform layer
ISCEV	International Society for Clinical Electrophysiology of Vision
MD	Mean Deviation
μV	Microvolts
ms	Milliseconds
OCT	Optical coherence tomography
ONH	Optic nerve head
ONL	Outer nuclear layer
OPL	Outer plexiform layer
PERG	Pattern electroretinogram
PhNR	Photopic negative response
PLSD	Protected Least Significant Difference
RPE	Retinal pigment epithelium
RGCs	Retinal ganglion cells
RNFL	Retinal nerve fiber layer
r/s	Reversals per second

SAP	Standard automated perimetry
SDE	Standard deviation error
TTX	Tetrodotoxin
UF-ERG	Uniform field electroretinogram
VF	Visual field
WHO	World Health Organization

Acknowledgment

A sincere appreciation goes to my thesis supervisor Dr. Stuart G. Coupland. The door to Dr. Coupland's office was always open whenever I had a concern about my project or the writing of the thesis. He consistently encouraged me to explore more aspects of my research but guided me in the right direction. I cannot express enough thanks and appreciation to my committee for their continued support and encouragement: Dr. Catherine Tsilfidis, my Co-supervisor; Dr. Garfield Miller; and Dr. Rustum Karanjia. I offer my truthful appreciation for the learning opportunities provided by my committee.

I am grateful for the help and time of all the people with whom I had the pleasure to work during the period of my Master's program, with a special mention to Dr. Emma Bondy-Chorney for her unfailing support and assistance in the past two years. I am also grateful to Kantungane Ange-Lynca and the hospital staff at the General and Riverside campuses of the Ottawa Hospital for their unfailing support and assistance in the research recruitment process. My family support was essential to accomplish my project. I want to thank my parents and my siblings. A special appreciation to my brothers and sister, Abdullah, Khaled and Rima, for their continuous support and encouragement. Importantly, I thank my loving and supportive husband, Madghis. Your help when the times got rough is much appreciated and appropriately noted. I offer you my heartfelt thanks. Finally, I would thank my bright children, Sedrin and Oumissa, who provide constant inspiration.

1-Introduction

1.1 The Retina

The retina covers the inner lining of the eye between the choroid and the vitreous (Figure 1.A). Histologically, the retina consists of two primary layers, the retinal pigment epithelium (RPE), and the neural layer (Figure 1.B). The outermost layer of the retina is the RPE (la Cour and Ehinger, 2005; Tortora, 2012). The neural retinal layer is in contact with the RPE and is itself composed of several layers. These layers include the outer segment, outer nuclear layer (ONL), outer plexiform layer (OPL), inner nuclear layer (INL), inner plexiform layer (IPL) and the ganglion cell layer (GCL). The retinal ganglion cell (RGC) bodies form the GCL, and their axons make the retinal nerve fiber layer (RNFL) (la Cour and Ehinger, 2005; Remington, 2012; Tortora, 2012). Approximately, 66%-75% of cells residing in the GCL are RGCs, and amacrine cell bodies occupy the remaining space. RGC axons converge at the posterior part of the eye to form the optic nerve head (ONH) and exit the eye through the lamina cribrosa to form the optic nerve. The lamina cribrosa is a mesh-like structure which is vulnerable to the stresses imposed by intraocular pressure (IOP) in terms of compression, distortion, and transformation (Figure 2.I.A), (Michelessi et al., 2015; Quigley, 2011; Tortora, 2012; Weinreb et al., 2014).

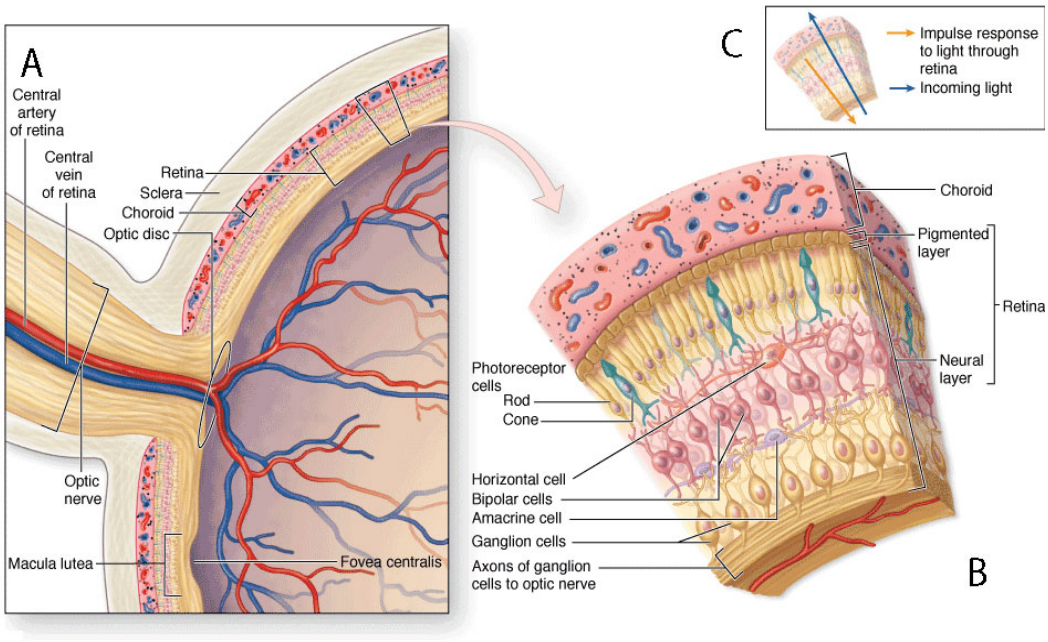

Figure 1: Layers of the retina

The figure shows a detailed structure of the back of the eye. (A) Cross section in the posterior part of the eye showing the retina and the optic nerve. (B) Magnification of the retina, showing the different retinal layers. (C) Light traverses the different layers of the retina (blue arrow) and generates an electrical signal (yellow arrow) that originates in the photoreceptors of the outer nuclear layer and is transmitted through the different layers of the retina and ultimately through the optic nerve to the brain (Mescher, 2016).

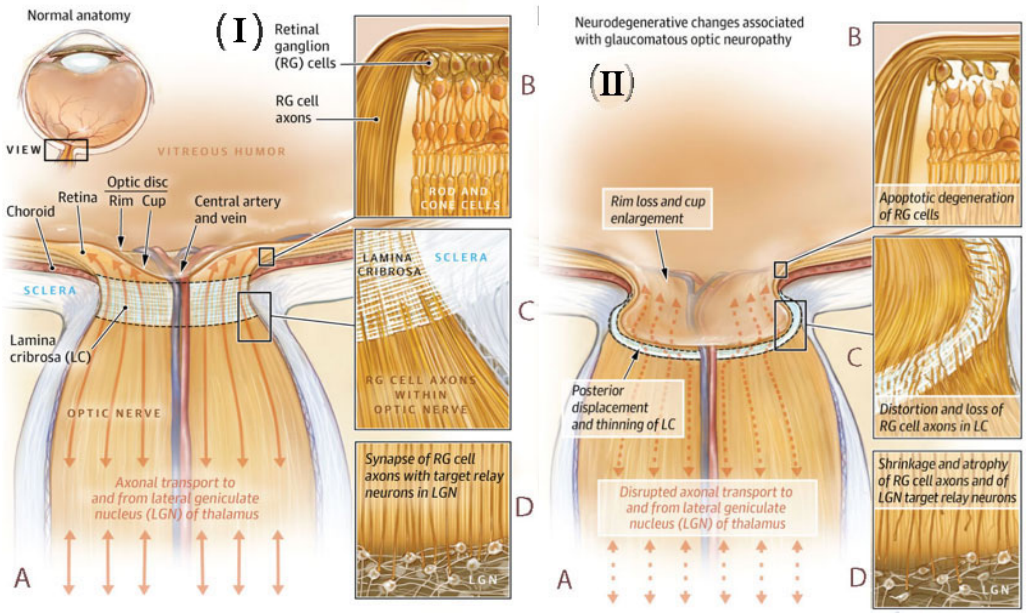

Figure 2: Cross section of the optic nerve and the retinal ganglion cells in a healthy eye (I) and in an eye with neurodegenerative effects due to glaucoma (II)

(I)-(A) Detailed illustration of the optic disc and optic nerve. (B) RGCs in the GCL send their axons along the nerve fiber layer and into the optic nerve. (C) RGC axons traverse the lamina cribrosa to enter the optic nerve. (D) RGC axons ultimately synapse with neurons in the Lateral Geniculate Nucleus (LGN). (II)-(A) Glaucomatous changes are shown in the optic disc and optic nerve, including enlargement of the optic cup and compression and thinning of the lamina cribrosa. (B) RGC degeneration is evident at the edge of the optic disc (C) Distortion, and compression at the lamina cribrosa leads to loss of RGC axons. (D) Degeneration of LGN due to changes in RGCs axons (Weinreb et al., 2014).

E 1.2 Glaucoma

Glaucoma is considered as a long-term neurodegenerative disease (Davis et al., 2016; Jonas et al., 2017; Sharma et al., 2008) with different underlying causes that leads to permanent blindness (Davis et al., 2016; Dong et al., 2016; Jonas et al., 2017; King et al., 2013; Sharma et al., 2008). It is characterized by slow degeneration of RGCs that leads to changes in the ONH and the RNFL (Dong et al., 2016; Jonas et al., 2017; Nickells, 2012; Oddone et al., 2016; Sharma et al., 2008). The optic nerve head (also referred to as the optic disc) is composed of a rim and a shallow cup in the normal eye (see Figure 2.I.A). As RGCs degenerate in glaucoma, this leads to thinning of the RNFL and to increased 'cupping' of the ONH (Harwerth et al., 2010; Sharma et al., 2008).

1.2.1. Pathophysiology

Glaucoma begins when the connection between the RGC axon and the RGC body is affected either by a mechanical force or a vascular insufficiency; consequently, RGCs will atrophy (Figure 2.II.B) (Bach and Hoffmann, 2008; King et al., 2013). As a result, the RNFL declines in thickness and the cup to disc ratio increases (Figure 2.II.A). It has been suggested that high IOP affects the RGC axons before affecting the RGC body (Nickells, 2012). Therefore, RGC axons lose their function, and this leads to the degeneration of the RGC bodies (Figure 2.II.D) (Nickells, 2012; Weinreb et al., 2014). About 1.5 million RGCs reside in the human retina. These cell counts drop by 0.4% annually due to aging, while glaucoma patients experience a 4% annual loss rate (Davis et al., 2016).

1.2.2. Risk factors

The anterior, as well as the posterior chambers of the eye, are filled with the aqueous humor fluid which is produced by the ciliary body (Figure 3.A). Aqueous humor passes through the pupil and drains through the trabecular meshwork that is situated at the iridocorneal angle. Any disturbance of the aqueous fluid outflow leads to elevated IOP (Figure 3.B.C) (Distelhorst and Hughes, 2003).

Elevated IOP is considered the most significant risk factor for glaucoma. Age, sex, and ethnic background can also affect the progression of the disease (King et al., 2013; Randall and Melton, 2004; Von Thun Und Hohenstein-Blaul et al., 2017, 2017). It is believed that glaucoma can develop through a combination of different risk factors at the same time (Von Thun Und Hohenstein-Blaul et al., 2017).

1.2.3. Classification of glaucoma

Glaucoma can be classified into two major groups (Weinreb et al., 2014) based on the anatomical changes in the drainage system at the iridocorneal angle (Figure 3.A) (King et al., 2013). The first group is called open-angle glaucoma (Figure 3.B), while the second group is called angle-closure glaucoma (Figure 3.C) (Weinreb et al., 2014). Both groups can also be classified as primary glaucoma without underlying causes. Secondary glaucoma can be caused by different conditions, including trauma, inflammation, tumor or medications such as corticosteroids (King et al., 2013; Weinreb et al., 2014).

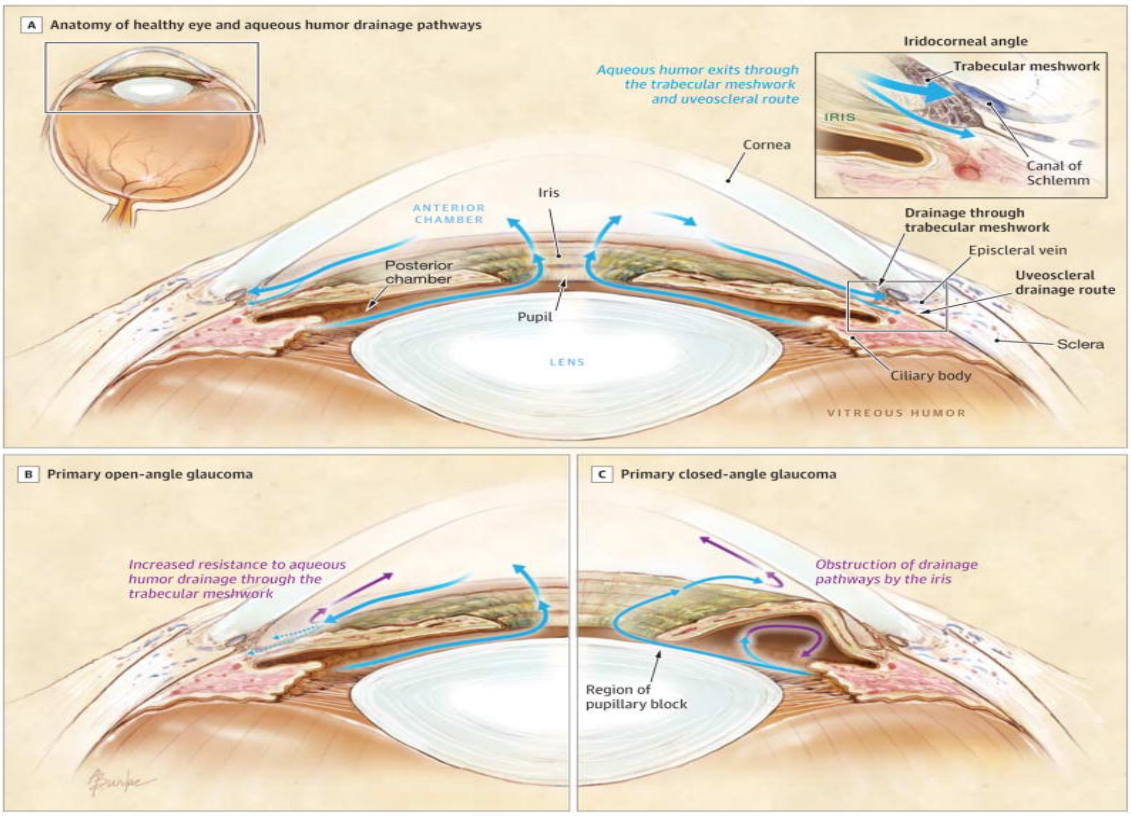

Figure 3: The drainage pathway of the aqueous humor in a healthy eye (A), (B) open-angle glaucoma, and closed-angle glaucoma (C)

(A) Aqueous humor is excreted by the ciliary body, flows through the pupil and is drained through the trabecular meshwork in a healthy eye. (B) In open-angle glaucoma, the iridocorneal angle is open, but there is a limited outflow of aqueous humor through the trabecular meshwork. (C) In closed-angle glaucoma, the drainage pathway is obstructed, preventing aqueous humor outflow (Weinreb et al., 2014).

1.2.3.1. Open-angle glaucoma

In open-angle glaucoma, the iridocorneal angle looks normal (King et al., 2013), but there is a dysfunction in the drainage system, which causes aqueous outflow impairment and IOP upsurge (Figure 3.B) (Distelhorst and Hughes, 2003; King et al., 2013). The progression of primary open glaucoma is slow, and it might take years to be symptomatic at the late stage (King et al., 2013). For this reason, the majority of the patients do not know that they have the disease and it goes untreated for long periods before diagnosis (Von Thun Und Hohenstein-Blaul et al., 2017).

1.2.3.2. Angle-closure glaucoma

In angle-closure glaucoma, the anterior chamber is closed by the iris, so the aqueous humor cannot access the drainage system as it accumulates behind the iris and pushes the iris forward, which causes angle closure (Figure 3.C) (Distelhorst and Hughes, 2003; King et al., 2013; Patel and Patel, 2014; Weinreb et al., 2014). Similar to open-angle glaucoma, angle-closure glaucoma is primarily a silent disease without any symptoms until it reaches an advanced stage (Weinreb et al., 2014). However, in some patients, it can present as acute angle closure and be associated with pain and other ocular symptoms. The main risk factors for angle-closure glaucoma are female gender and Asian ethnicity. Furthermore, there are structural ocular risk factors, including shallow anterior chamber depth, thicker forward positioned lens, and short axial length (Patel and Patel, 2014; Weinreb et al., 2014).

1.2.4. Prevalence

Glaucoma is the second leading cause of blindness worldwide (Dong et al., 2016). It is speculated that about 70 million people globally have been diagnosed with glaucoma, and 10% of them are bilaterally blind (Weinreb et al., 2014). In the United States, approximately 2.5 million are affected by glaucoma, and 50% of them are unaware that they have the disease (Distelhorst and Hughes, 2003; Mantravadi and Vadhar, 2015). Primary open-angle glaucoma is the most common type in the Western world (Von Thun Und Hohenstein-Blaul et al., 2017), and it is estimated that 5.3 million people will be blind due to open-angle glaucoma by 2020 (Patel and Patel, 2014). Although the incidence of primary open-angle glaucoma is more common than primary angle closure glaucoma by a factor of six, the rate of bilateral blindness is higher in primary angle closure glaucoma (Jonas et al., 2017). Early glaucoma changes are indistinct, and practitioners find it challenging to define (Michelessi et al., 2015). Therefore, finding a reliable diagnostic method that has the ability to detect early glaucomatous changes would help clinicians and patients in terms of management and outcome (Quigley, 2011).

1.2.5. Diagnosis

Glaucoma diagnosis relies on using a test that can recognize and measure vision abnormality as well as an RNFL defect (Harwerth et al., 2010). Although glaucoma detection necessitates comprehensive examination for both optic nerve disc and visual field (VF) changes, the majority of tests are considered inadequate to detect glaucoma (Von Thun Und Hohenstein-Blaul et al., 2017). Therefore, the majority of patients can have

glaucoma for more than a decade without being aware of it, and about 50% of the RGCs and axons can be lost before any detectable pathological changes occur (Von Thun Und Hohenstein-Blaul et al., 2017).

Assessing VF by standard automated perimetry (SAP) is the classical way to diagnose and determine the advancement of glaucomatous neuropathy, but recently optical coherence tomography (OCT) has become the standard method (Harwerth et al., 2010). Both methods rely on comparing the result with an age-matched standard database, which can give an idea about RGC death. However, it is not enough to determine the stage of the disease (Harwerth et al., 2010).

1.2.5.1. Standard automated perimetry (SAP)

Standard automated perimetry (SAP) is used to detect VF defects by evaluating the visual function of RGCs by assessing light sensitivity (Harwerth et al., 2010; Mavilio et al., 2015). It is considered the gold standard method for detecting the functional defect in glaucoma (Parikh et al., 2008). VF defects appear when there is any abnormality in the visual sensory pathway from the retinal photoreceptors to the visual cortex (Cassin, 1995). Moreover, SAP can detect glaucomatous defects only when 30-40 % of nerve fibers are lost (Dong et al., 2016; Mavilio et al., 2015). A typical printout from the SAP test is shown in Figure 4. The results contain general information about the patient and the test itself and show different patterns and plots for VF evaluation (Heijl and Patella, 2002).

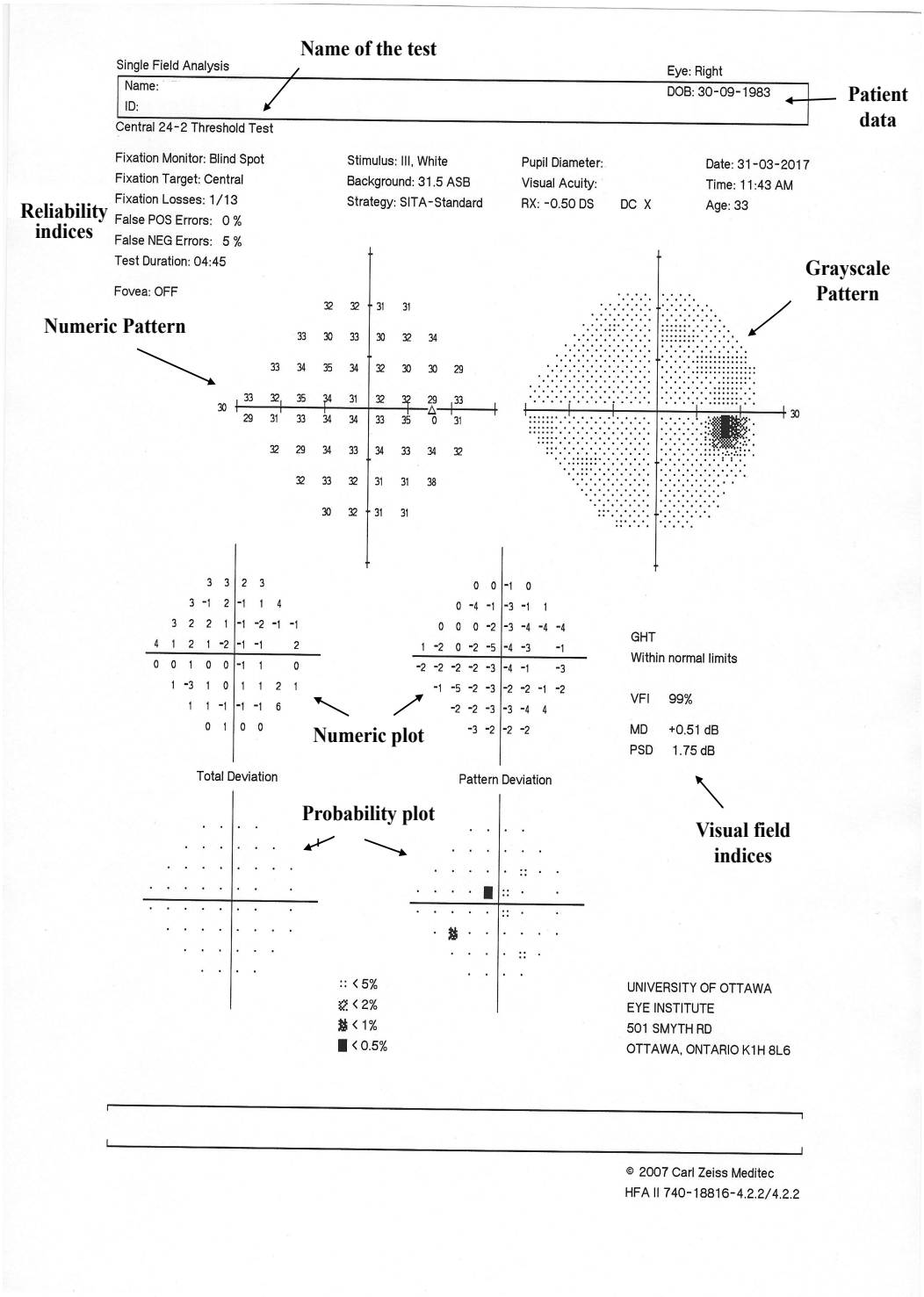

Figure 4: Visual field result for the standard automated perimetry for the right eye of a healthy subject

The report shows different patterns and plots for VF evaluation. The Numeric pattern assesses retinal light sensitivity in decibels. The Grayscale pattern demonstrates the result in dark and light grayscale to demonstrate low and high light sensitivity, respectively. The numeric plot showing total and pattern deviation represents the results for the patient in terms of deviation from the normal standard data based on an age-matched control and as an identified defect in VF, respectively. Probability plot in terms of total and pattern deviation shows the places outside the normal and represents the results after removing any generalized defects. Reliability indices are used to make sure that the results are Quantified (Yaqub, 2012). VF indices give an idea about the degree of deviation from the normal field regarding values and shape by measuring mean deviation (MD) and pattern standard deviation (PSD). The above example is modified from a healthy volunteer medical report at the University of Ottawa Eye Institute.

1.2.5.2. Optical coherence tomography (OCT)

Optical coherence tomography (OCT) was introduced into the clinical setting in 1991 (Dong et al., 2016; Leung, 2014) and since that time it has been used for detection of both glaucomatous damage and progression (Leung, 2014). OCT is a noninvasive tool with a high-resolution image (Denniston and Murray, 2006; Dong et al., 2016; Podoleanu, 2012) that can be produced as a cross-sectional image during the test (Dong et al., 2016; Podoleanu, 2012). OCT can visualize the retinal microstructure with a spatial resolution of 2-3 microns (Figure 5.B) as well as the pathology of the retina (Figure 6.A, B) without taking a specimen (Wolfgang and Fujimoto, 2015). Recently, it was shown that OCT could detect abnormal RNFL thickness before VF defects appear, with a specificity of 95% (Harwerth et al., 2010; Mavilio et al., 2015). Although OCT is well established in clinical practice, and it gives an objective assessment of RGCs by calculating RNFL thickness (Figure 5.C, 6.C) (Harwerth et al., 2010; Mavilio et al., 2015), OCT cannot detect RNFL changes in advanced glaucoma, and the lowest reading that can be detected by OCT is 30 μm even in end-stage glaucoma with no light perception (Leung, 2014).

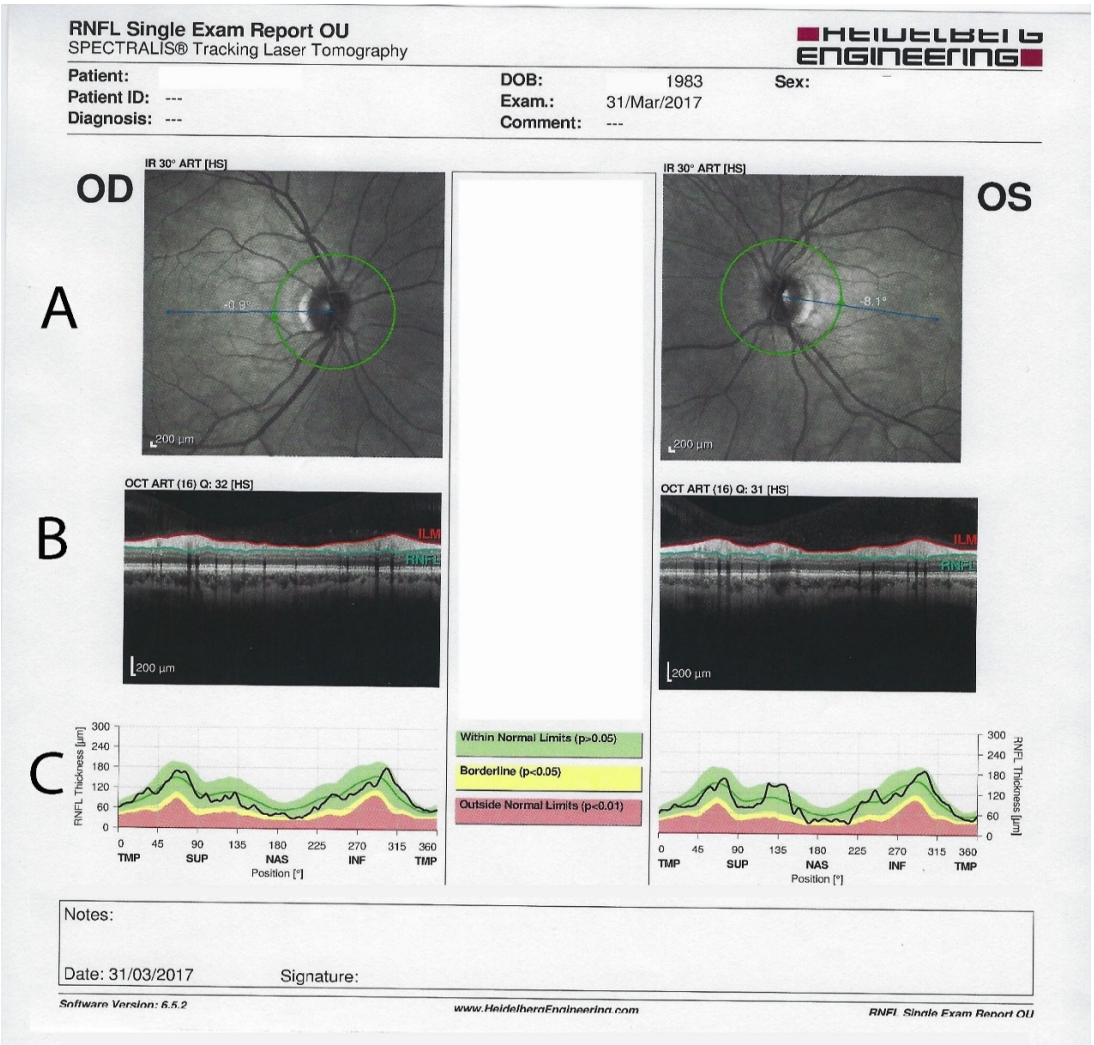

Figure 5: OCT report for the right and the left eyes of a healthy subject

(A) Images identify the site of the scan around the optic disc in the right eye (OD) and left eye (OS). (B) Cross section of the retina shows the retinal layers. (C) Black line demonstrates the normal range of RNFL thickness in each region and compares it with normative data. Images are modified from a healthy subject medical record at the University of Ottawa Eye Institute.

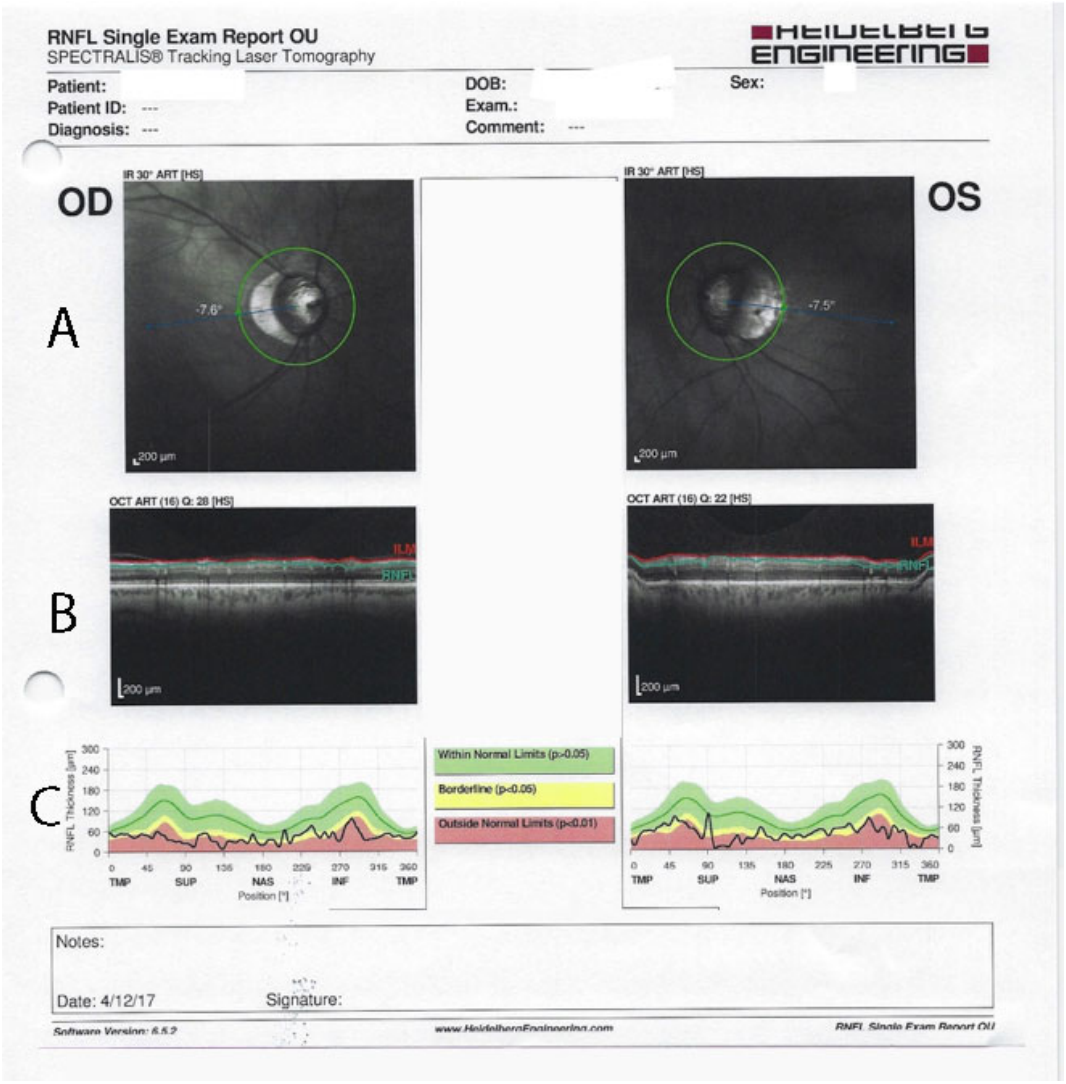

Figure 6: OCT report for a glaucoma patient for the right and the left eyes

(A) Images show optic nerve head cupping. (B) Cross sections of the retina reveal changes in the retinal layers (C) Black line shows that RNFL thickness is below the normal range. Images modified from a medical record of glaucoma patient at the University of Ottawa Eye Institute.

1.2.6. Management

The main aims of glaucoma treatment are delaying the advancement of the disease and stabilizing the quality of life (Schuman et al., 2004; Weinreb et al., 2014). The only established way to treat glaucoma is to lower the elevated IOP through pharmacological or surgical means (Von Thun Und Hohenstein-Blaul et al., 2017; Weinreb et al., 2014). Moreover, it has been proposed that a reduction of as little as 1mmHg of IOP would reduce the risk of glaucoma progression by 10%-19% (Schuman et al., 2004).

1.3. Electroretinography (ERG)

Electroretinography provides an objective measure of retinal function by recording the retinal electrical response to a flashing light stimulus (Carpi and Tomei, 2006; Heckenlively and Arden, 2006; Wilsey and Fortune, 2016). The first ERG was recorded in 1865 by Swedish physiologist Holmgren on a frog (Jampol, 2001; Wachtmeister, 1998). Although the first electrophysiological human recording was carried out in 1877, clinical use of the ERG was not widespread until 1941 (Jampol, 2001).

Clinical application of electroretinography has shown a significant improvement due to upgrades in the technology for ERG recording in the clinical setting, as well as an increased understanding of the relationship between the generation of the specific ERG components by specific retinal neurons (Heckenlively and Arden, 2006). Electroretinography started to be adopted in the middle of the twentieth century. At that time, comparing the data recorded at different sites was challenging since the ERG tests

were recorded under different conditions (Heckenlively and Arden, 2006). The International Society for Clinical Electroretinography of Vision (ISCEV) was aware of the importance of the standardization of the recording procedure, and the first clinical ERG standard was published in 1989 (Heckenlively and Arden, 2006). The Society developed the ISCEV standards to address different parameters of electroretinography including stimulation, electrodes, types of recording equipment, recording protocols, analysis and reporting results (Bach et al., 2013; Korth et al., 1993). Given that the components of the ERG response are representative of the activities of the various retinal layers (Korth, 1997; Smith et al., 2017; Wachtmeister, 1998; Wilsey and Fortune, 2016), the function of RGCs can be evaluated using ERG (Porciatti, 2015).

1.3.1. Types of Electroretinography

1.3.1.1. Pattern Electroretinogram (PERG)

The pattern electroretinogram (PERG) is one of the electrophysiological methods that has been adopted to assess the performance of RGCs in humans and animals (Fiorentini et al., 1981; Mafei and Fiorentini, 1981; Ventura et al., 2005). The PERG is a noninvasive method that records the retinal response to a unique type of stimulus that takes the shape of a black and white checkerboard (Figure 7.A) or bars (Figure 7.B) that reverses throughout the test with constant mean luminance (Jampol, 2001; Kreuz et al., 2014; Lam, 2005; Luo and Frishman, 2011; Porciatti, 2015; Wilsey and Fortune, 2016).

The frequency of the stimulus is 1-8 Hz which is 2-16 reversals per second (r/s) (Bach and Hoffmann, 2008; Luo and Frishman, 2011; Miura et al., 2009). The PERG waveforms consist of three components (Figure 8). The first component is a small negative wave that peaks at 35ms (N35), the following one is a positive peak at 45-60 ms (P50), and the last component is a negative trough that can be detected at 90-100 ms (N95) (Figure 8) (Bach et al., 2013; Jampol, 2001). It is well known that P50 reflects the activity of both RGCs and other retinal cells, while the N95 response mainly detects RGC performance (Berninger and Schuurmans, 1985; Lam, 2005; Schuurmans and Berninger, 1985).

In 1982, May et al. published the first article regarding the use of the PERG in glaucoma patients (Bach and Hoffmann, 2008; May et al., 1982) and since that time many researchers have detected glaucoma-related RGC dysfunction based on changes in the amplitude and timing of the waveforms (Kreuz et al., 2014; Roy et al., 1997).

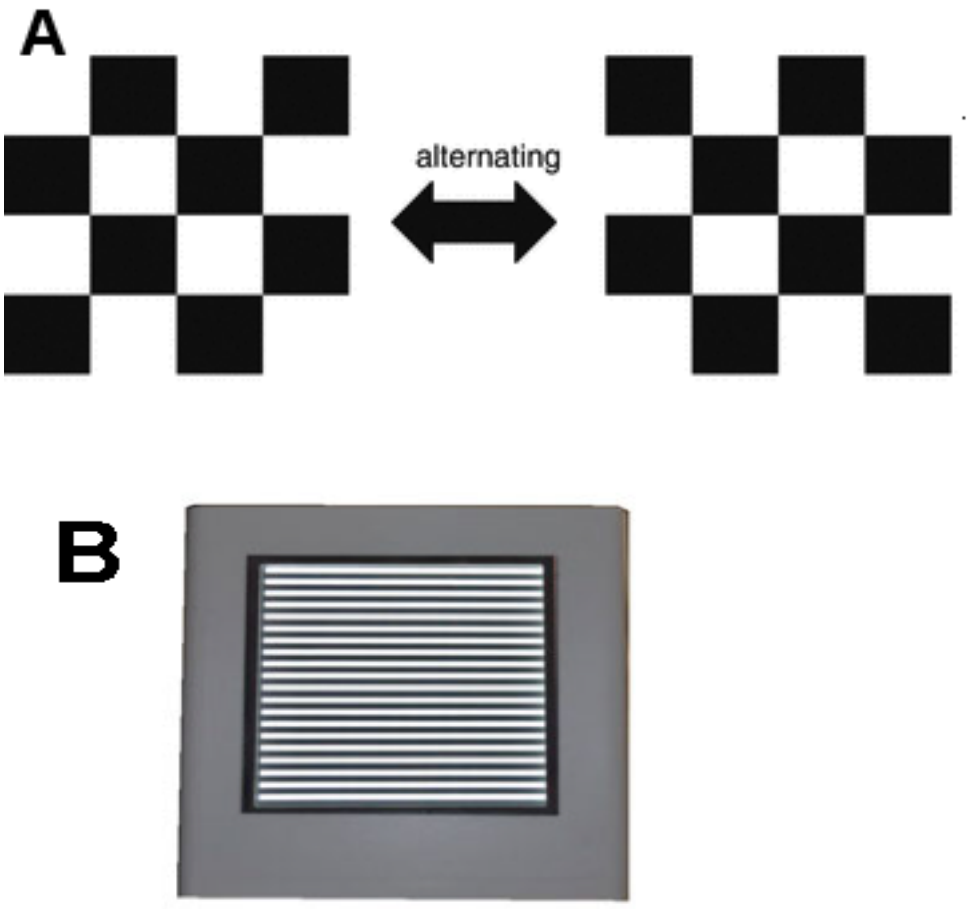

Figure 7: PERG checkerboard and bars stimuli

(A) The shape of the checkerboard stimulus in the alternating positions period (B) Similar to the checkerboard stimulus, the bars stimulus also alternates between light and dark bars. The images are modified from (Skalicky, 2016).

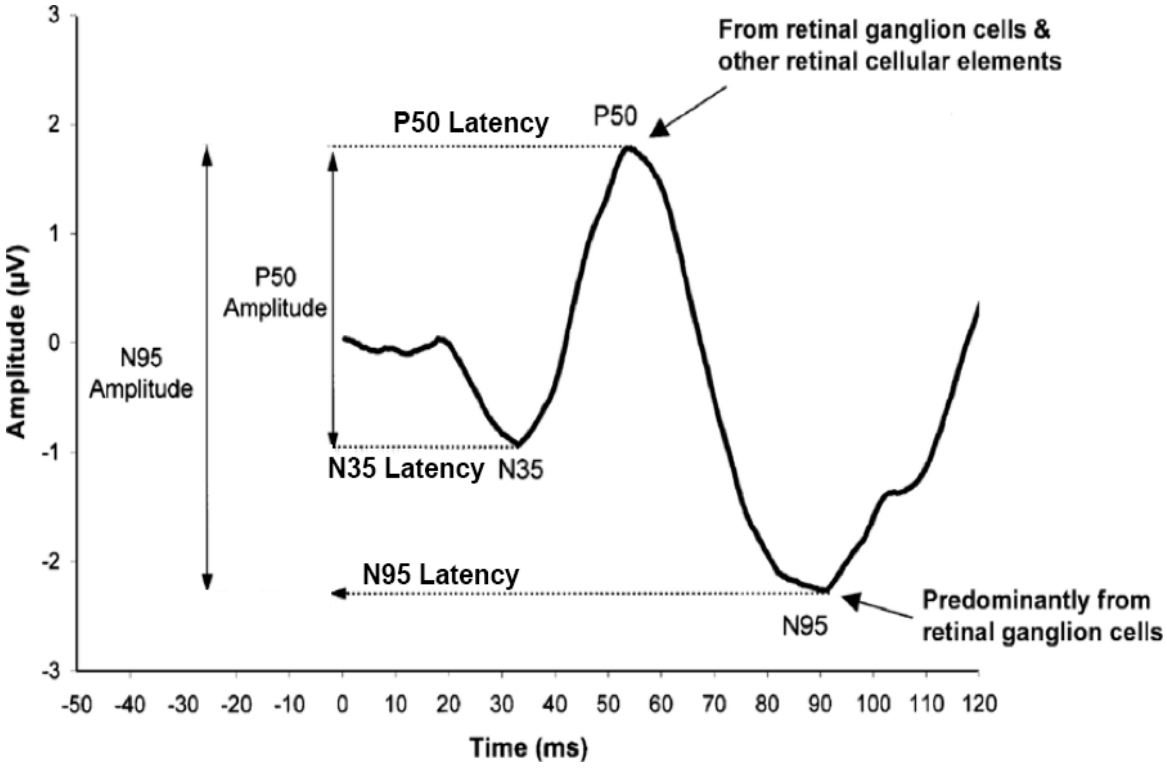

Figure 8: PERG waveforms

Classical PERG waveforms are showing the N35, P50, and N95 components and identifying the cell origin of the P50 and P95 components. The images are modified from (Lam, 2005).

A partial decrease in the P50 response and a considerable drop in the N95 response was achieved in non-human primates following an intravitreal injection of tetrodotoxin (TTX), which is a substance that blocks RGC action potentials (Lam, 2005; Viswanathan et al., 2000). Moreover, induced glaucoma in non-human primates revealed a decrease in the amplitude of P50 and N95 which was accompanied by histological findings showing RGC damage (Johnson et al., 1989; Kreuz et al., 2014; Marx et al., 1986).

Based on the advancements in PERG technology (Bach and Hoffmann, 2008), it is believed that the PERG has the potential to detect early glaucomatous damage with minimal VF defects (Bach et al., 2006; Hood et al., 2005; Luo and Frishman, 2011) and in patients with normal VF results (Bach and Hoffmann, 2008; Ventura et al., 2005). Furthermore, Banitt et al. found that glaucoma suspect patients with PERG amplitudes of $\leq$ 50% of the normal collected data had an increased chance of having a high deterioration rate in their RNFL thickness over the five year study period, which emphasizes the need for early intervention (Banitt et al., 2013; Jampol, 2001). PERG shows changes not only in clinically manifested glaucoma patients (Trick, 1992; Ventura et al., 2005; Wanger and Persson, 1983) but also in those patients with early glaucomatous changes (M. Bach, 2001; Sehi et al., 2010; Ventura et al., 2005).

It is strongly believed that PERG clinical recordings should be based on ISCEV standards to ensure reliable results (Bach et al., 2013). ISCEV has not published any standard international ranges for PERG components primarily due to different clinical ERG instrumentation parameters producing different ranges of amplitude and timing of PERG

components. Consequently, each lab should have normative data based on their equipment and population (Bach et al., 2013).

1.3.1.2. Full-Field Electroretinogram

The full-field electroretinogram is commonly used for retinal function testing and represents the activity of the entire outer retina in response to light flashes that are generated in a Ganzfeld dome (Birch DG and Anderson JL, 1992; Frishman et al., 1996; Lam, 2005; Sieving et al., 1986). Full-field ERG started to be used in the clinical setting in the 1940s, and in 1989 ISCEV published standards for full-field ERG recording (Lam, 2005; Marmor and Zrenner, 1998).

The uniform field electroretinogram (UF-ERG) is a particular type of full-field ERG that uses a single flash stimulus with a light background (Lam, 2005; Viswanathan et al., 2000). Primary research in the Frishman laboratory at the University of Houston with non-human primates using pharmacological blockage of spiking activity of the inner-retinal neurons demonstrated the role of RGCs in generating the photopic negative response (PhNR) (Holder, 1987; Viswanathan et al., 2000). Moreover, in the Frishman lab, a modified PhNR was developed by using UF-ERG with a long duration stimulus (200 ms) (Figure 9.A) (Viswanathan et al., 1999). The long duration stimulus produces two separate responses, the $PhNR_{on}$ and $PhNR_{off}$ responses, that come after b-wave and d-wave at light onset and light offset, respectively (Figure 9.A) (Evers and Gouras, 1986; Frishman et al., 2018; Sieving et al., 1994; Viswanathan et al., 1999, 2000). Additionally, a short duration stimulus (≤ 5ms), in the form of brief flashes, produces a- and b-waves followed by a

negative response PhNR, in which $PhNR_{on}$ and $PhNR_{off}$ responses are essentially superimposed due to much shorter stimulus duration (5ms vs. 200 ms). (Figure 9.B) (Viswanathan et al., 1999, 2000).

The a-wave reflects the activity of cone photoreceptors (Heynen and van Norren, 1985; Viswanathan et al., 2001) and the b-wave represents the activity of cone bipolar cells (Sieving et al., 1994; Viswanathan et al., 2001). The PhNR is a slow negative response that comes after the b-wave as a result of cone stimulation by single flash using full-field ERG (Wilsey and Fortune, 2016) that reflects the function of RGCs as well as their axons in both humans and non-human primates (Frishman et al., 2018; Kinoshita et al., 2016; Viswanathan et al., 1999, 2000, 2001). Recently, ISCEV has published a protocol for full field PhNR recording, which includes the recommended stimulus parameters (Frishman et al., 2018).

A relation between the response from both PERG and UF-ERG had been recorded from experimental glaucoma, and it is believed that the response is related to a decrease in the spiking activity of RGCs as well as their axons (Holder, 1987; Viswanathan et al., 2000). Electrical activities within RGCs and optic nerve do not contribute to generating a- or b-waves. Therefore, glaucoma which mostly affects RGCs does not diminish ERG a-wave or b-wave amplitudes (Fishman, 1985; Viswanathan et al., 1999).

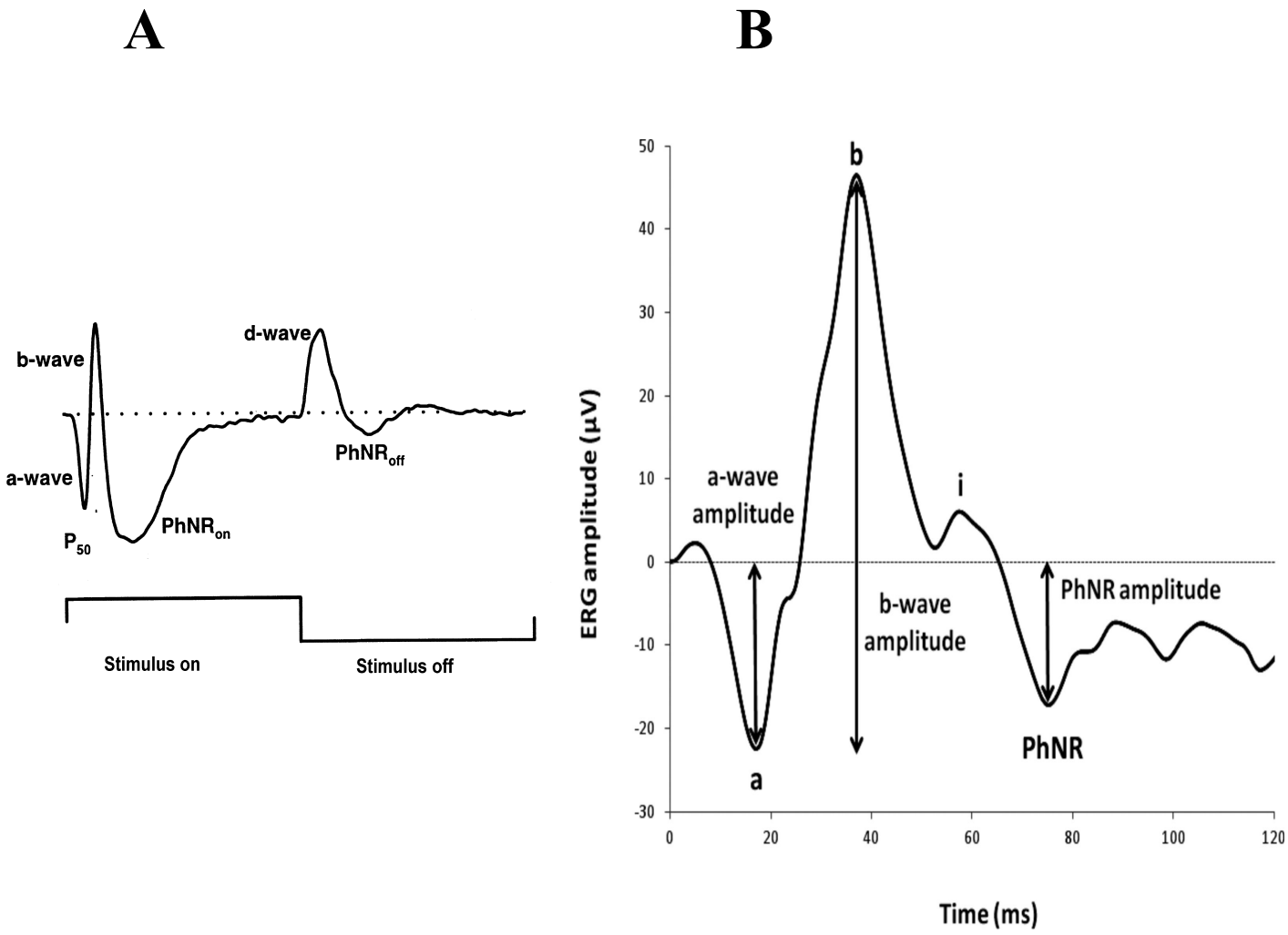

Figure 9: Uniform field ERG waveforms resulting from a long duration stimulus (A) and from a short duration stimulus (B)

(A) The classical uniform field waveforms with $PhNR_{on}$ and $PhNR_{off}$ responses to long duration stimulus. The image is modified from (Viswanathan et al., 2000). (B) The uniform field ERG waveforms (a-, b- waves and PhNR) generated using a short duration stimulus (5 ms). The image is modified from (Viswanathan et al., 2001).

Pattern ERG studies have been recorded in the laboratory for decades, and the research literature has shown their value in early detection of RGC dysfunction related to glaucoma (Bach and Hoffmann, 2008; Wilsey and Fortune, 2016). Unlike the PERG, the PhNR is produced by a flash stimulus and also reflects RGC function in glaucoma (Wilsey and Fortune, 2016). Since PhNR is not affected by image clarity or steady fixation, it has significant advantages in the clinical setting and is becoming the preferred test in the laboratory.

The changes in PERG and UF-ERG responses produced by experimental glaucoma are related and were found to be mainly a consequence of reduced spiking activity of RGCs and their axons. These findings suggest that UF-ERG could serve as a useful alternative to PERG in the assessment of clinical glaucomatous neuropathy (Viswanathan et al., 2000). To date, there are no published results related to the recording of UF-ERG in patients with glaucoma, and investigating this will be the main focus of this thesis.

1.4. Hypothesis and Objectives:

1.4.1. Description of rationales and hypotheses

The following study was carried out at the University of Ottawa Eye Institute. This study investigated the potential of using the Diagnosys D-341 Attaché-Envoy Electrophysiology System to conduct PERGs and UF-ERGs to detect early changes in glaucoma, and to determine the sensitivity and specificity of these tests as a diagnostic tool. In order to investigate this, we included patients at two different stages of glaucoma disease progression as well as a control group. We examined the changes in PERG and UF-ERG parameters related to glaucoma in terms of a decrease in the amplitude, a delayed time component of the response, and the sensitivity and the specificity of both techniques.

1.4.2. The role of PERG and UF-ERG in glaucoma detection

SAP and OCT are well established in the clinical setting as diagnostic tools to detect glaucomatous changes in the form of VF defects and decrease in RNFL thickness. However, both methods are not able to detect early changes in glaucoma. RGC dysfunction and loss are the primary causes of vision loss and eventual blindness in glaucoma. PERG and UF-ERG parameters, specifically N95 and PhNR respectively, reflect RGC activities. Therefore, using PERG and UF-ERG would not only detect these changes in the early stage of glaucoma but would also help to monitor the disease progression. PERG is well established as a complementary diagnostic tool for retinopathy related to glaucoma and other retinal diseases. UF-ERG, on the other hand, is newly introduced to the field, but it

shows great promise for the detection of RGC dysfunction. It has been tested on non-human primates with experimental glaucoma, and the results were promising as PhNR amplitude appeared to be decreased with experimental glaucoma. Furthermore, it has been documented that PhNR amplitude is reduced in glaucoma patients compared to healthy subjects (Frishman et al., 2018; Viswanathan et al., 1999).

UF-ERG recording does not necessitate refractive correction or clear optics which are both advantages over PERG recording requirements. Here, we investigate the potential of using UF-ERG as a diagnostic tool and determine its sensitivity and specificity in glaucoma detection. We utilized a new technology developed by Diagnosys LLC, the D-341 Attaché-Envoy Electrophysiology System, which shows the advantage of being able to record both PERG checks and bars and UF-ERG in the same machine. Importantly, we followed the ISECV standards for both PERG, UF-ERG and PhNR of UF-ERG.

1.4.3. Hypotheses

The hypotheses are:

1) UF-ERG and PERG amplitudes will be decreased in glaucoma patients and will vary with disease progression, and

2) the newer technology of UF-ERG will show equal or increased sensitivity and specificity for detection of glaucoma compared to PERG.

2-Material and Methods

This research is part of a larger clinical protocol which is a prospective, interventional device study (#20160190 – Incorporation of the Diagnosys D-341 Attaché-Envoy Electrophysiology Systems into the Clinical Setting), which was approved by the Ottawa Health Science Network Research Ethics Board (OHSN-REB) and was conducted at the University of Ottawa Eye Institute**.** The research took place at the University of Ottawa Eye Institute during the period from September 2017 to October 2018 on 50 glaucoma patients (29 male and 21 female), including 41 glaucoma suspect eyes and 59 eyes with confirmed glaucoma who were diagnosed based on a clinical examination and the results of both SAP and OCT.

The patients were recruited from the glaucoma clinic at the Ottawa Hospital General and Riverside Campuses. Thirty-six normal control eyes (4 males and 14 females) that ranged in age from 20 – 75 years, who had IOP of 21mmHg or less with no history of high IOP were recruited by volunteer staff and family members. The recruited glaucoma subjects ranged in age from 20 to 87, and they had a visual acuity of 20/30 or better for each eye, and the test was done without pupil dilation. In this study, a comprehensive ocular exam was done on glaucoma patients by a senior ophthalmic resident or ophthalmologists in the clinic. PERG and UF-ERG were performed on both control and glaucoma subjects, while OCT and SAP were done on glaucoma subjects only.

2.1 Humphrey field analyzer 24-2 automated perimetry

VF evaluation was done by using the Humphrey field analyzer II (Zeiss, Germany). Initially, each eye was examined separately to avoid the overlap from the other eye's field (Cassin, 1995). During the recording, the machine was used under SITA-Standard strategy with white size III stimulus and background illumination of 31.5 apostilbs (ASB) =10.03 cd/m^2. The patient was instructed to maintain fixation throughout the test and to examine an area of 24 degrees around the fixation point. Brief dim points of light with different thresholds were projected on the perimeter surface, and the patient responded to these stimuli by pressing a button. The luminance of these points was varied such that a threshold of detection was determined for each point. The data were collected and categorized as reliable and unreliable results based on reliability indices, and the unreliable results were repeated. The final result was presented as patterns and probability plots (Cassin, 1995; Heijl and Patella, 2002).

2.2 Spectral domain OCT

Glaucoma patients had spectral OCT tests with undilated pupils using either the Heidelberg HRA+OCT (Heidelberg Engineering, Heidelberg, Germany) or the Cirrus HD-OCT Model 500 (Carl Zeiss, Oberkochen, Germany). All potential glaucoma patients had a macular scan and RNFL thickness by the same instrument at the same session. The patient was asked to maintain fixation throughout the test. Spectral OCT used a source of light near the infrared spectrum to give a high-resolution cross-sectional image of the retina (Denniston and Murray, 2006). Patients who were examined on the Heidelberg HRA+OCT

system received a 3-D View Macular Raster Scan and the RNFL scan. Patients examined on the Cirrus HD-OCT had a 200x200 Macular cube and a 200x200 Optic Disk cube test.

2.3 Uniform field electroretinography

ERG was performed following the standard of the University of Ottawa Eye Institute clinical protocols. UF-ERG and PERG recordings were obtained with DTL micro conductive fiber electrodes (DTL-Plus™, Diagnosys LLC, Lowell, MA). Each electrode was placed across the lower bulbar conjunctiva at the limbal margin after administering one drop of ALCAINE® (proparacaine hydrochloride 0.5% w/v) in each eye. The ground electrode (535 Foam Electrodes, Kendall™) was placed on the frontal part of the right or left wrist after exfoliating the skin by Lemon Prep (Mavidon, Riviera Beach FL). Both electrodes were connected to the 32-bit amplifier electrode montage of the Envoy D352 (Diagnosys LLC, Lowell, M) ERG system. Visual stimulation for both UF-ERG, PERG, and PhNR was provided by an 800x600 pixel OLED stimulator (Diagnosys LLC Lowell, Ma). UF-ERG luminance modulation subtended a 24x32 degree viewing angle producing a luminance of 300 cd/m^2 for a 200 msec duration. 220 replications of 230 msec sweep duration were obtained at both stimulus onset and stimulus offset and averaged to produce the $PhNR_{on}$ and $PhNR_{off}$ response. The on- and off-PhNRs are averaged together to form the UF-ERG PhNR.

2.4 Pattern electroretinography

PERG was recorded by the same electrodes that had been used for UF-ERG PhNR recordings. Each eye was stimulated separately by using checkerboard followed by bars stimuli from the Diagnosys D-341 Attaché-Envoy Electrophysiology System (Diagnoysys LLC, Lowell, MA). The checkerboard stimulus had a mean luminance of 300 cd/m^2 with 100% contrast and 0.8° check size. The response was recorded at a pattern-reversal rate of 2 r/s. The bars stimuli had a mean luminance of 300 cd/m^2 with 100% contrast and a spatial frequency of 0.5 cycles per degree. A total of 150 sweeps of 250 ms sweeps duration for checks stimuli, and 100 sweeps for bars stimuli were recorded and averaged for each eye. The candidates were advised to keep fixation by looking at the center of the OLED screen throughout the recording and were given blink breaks to reduce noise. The results of both PERG and UF-ERG were presented as waveforms and were reviewed by an electrophysiologist (Dr. Stuart Coupland).

2.5 Statistical analysis

2.5.1 PERG P50 and N95 checks and bars and UF-ERG

PERG P50 and N95 amplitude and peak latency values for both checks and bars stimulation as well as UF-ERG waveform components of amplitude and peak latency were analyzed using Staview™ v.4.5 (Abacus Concepts), statistical analysis software. One way factorial analysis of variance (ANOVA) was performed comparing the control, glaucoma

suspects and glaucoma patients on the previously determined parameters. ANOVA main effects were determined using Fisher's PLSD with p-value <0.05. Post hoc analysis of group comparisons was then performed.

2.5.2 Sensitivity and specificity

The sensitivity and specificity calculations are based on comparing the new diagnostic test to the gold standard test. When this comparison is made, there are four possible outcomes identified, and these are shown in a two by two (2X2) table (Figure 10.A). The potential of the test to correctly identify patients that have the disease is defined as sensitivity, while the capability of the test to distinguish individuals who do not have the disease is known as specificity. Formulas for the calculation of sensitivity and specificity are found in Figure 10.B (Parikh et al., 2008).

A

	Gold standard disease present	Gold standard disease absent	
Test positive	True positives (TP)	False positives (FP)	Total test positives:
	a	b	a+b
Test negative	False negative (FN)	True negatives (TN)	Total test negatives:
	c	d	c+d
	Total diseased:	Total normal:	Total population:
	a+c	b+d	a+b+c+d

B

	Disease present	Disease absent
Test positive	a (TP)	b (FP)
Test negative	c (FN)	d (TN)
	Sensitivity:	Specificity:
	a/ (a+c)	d/ (b+d)

TP: True positive, FP: False positive, FN: False negative, TN: True negative

Figure 10: Two by two table to calculate the sensitivity and the specificity

(A) The figure shows the components of the 2X2 table based on the results of the gold standard test and the new diagnostic test. (B) Formulas for calculating the sensitivity and specificity of the new test are presented. (Parikh et al., 2008).

3-Results

3.1 Pattern Electroretinogram

In order to determine the effect of glaucoma on the PERG components, the two PERG tests (one using the alternating checkerboard pattern and the other using alternating bars) were carried out on the eyes of both glaucoma groups (N = 100) and the control group (N = 72). Glaucoma patients' eyes were classified into glaucoma suspect (N = 42), and glaucoma (N = 58) groups based on IOP and SAP results. The results of each of the two PERG tests were analyzed in order to determine if both tests were equally reliable at identifying glaucoma and glaucoma suspect patients.

3.1.1. PERG checks N95 amplitude and latency detect changes in glaucoma patients

The components of the PERG checkerboard test were recorded, and ANOVA revealed a trend in the P50 amplitude (Figure 11), although the trend did not reach significance. However, the N95 amplitude was significantly altered in the tested groups (P-value = 0.0014) (Figure 12). Moreover, Fisher's (PLSD) post-hoc analysis revealed a significant decrease in N95 amplitude between glaucoma suspect and control group (P-value = 0.0128) and glaucoma and control groups (P-value = 0.0006) (Figure 13). Similarly, ANOVA showed that the latencies of P50 and N95 components were affected in the experimental groups, and the results were statistically significant (P-values = 0.0009 and < 0.0001, respectively) (Figures 14, 15). Additionally, statistically significant results for the delay in

P50 latency were identified by Fisher's post-hoc analysis between glaucoma suspect and control groups (P-value = 0.0012) and glaucoma and control groups (P-value = 0.0020) (Figure 16).

With regards to N95 latency, a statistically significant increase in the time was identified by Fisher's post-hoc analysis between glaucoma suspect and control groups (P-value = 0.0001), and glaucoma and control groups (P-value < 0.0001) (Figure 17). Altogether, the data presented here suggest that PERG checks N95 amplitude and PERG checks for both P50 and N95 latency can detect changes related to glaucoma with a significant difference between glaucoma groups and the control group.

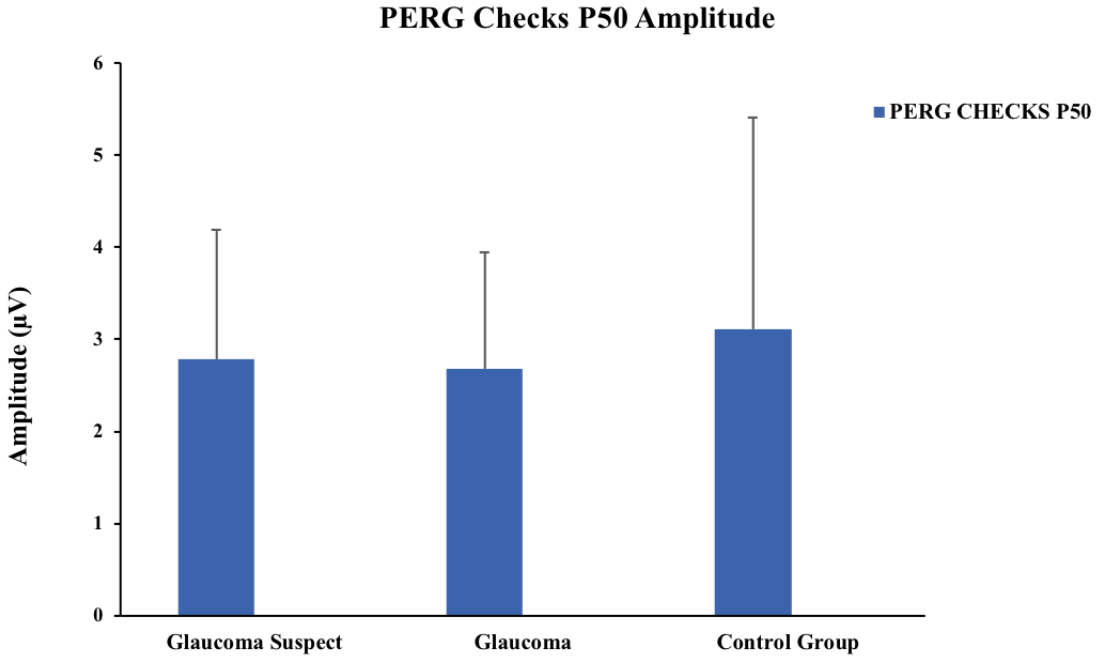

Figure 11: PERG checks P50 amplitude in the glaucoma groups and the control group

PERG checks P50 amplitude showed a trend with ANOVA in the tested groups, but this trend did not reach significance. Error bars represent SD.

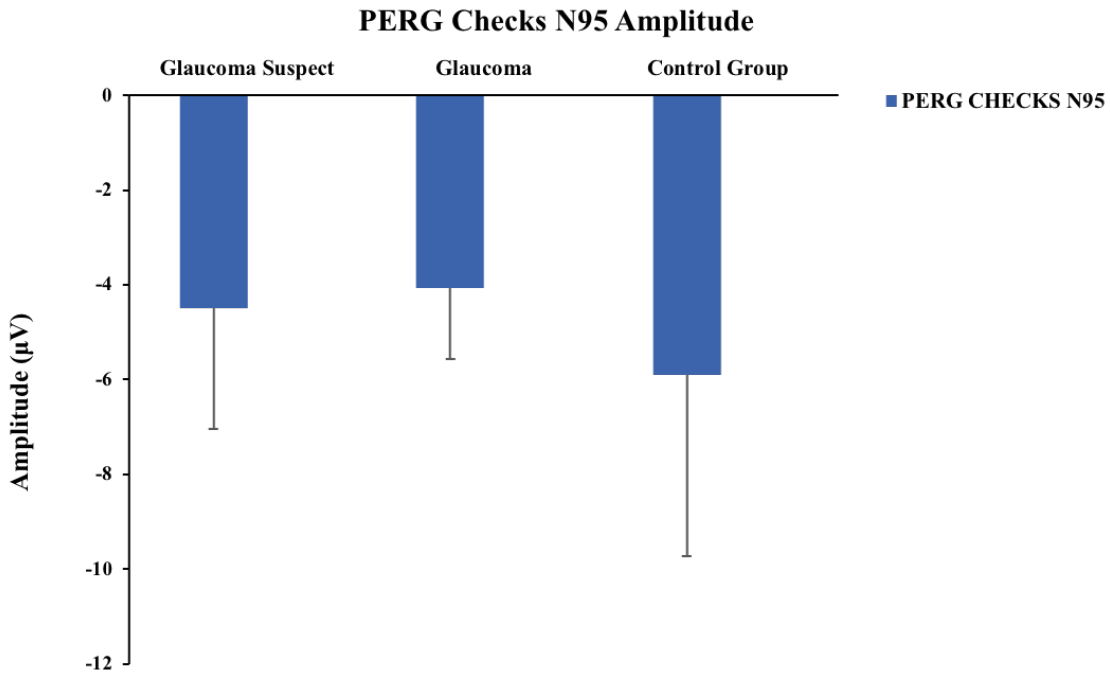

Figure 12: PERG checks N95 amplitude in the glaucoma groups and the control group

ANOVA detected a statistically significant difference in N95 amplitude between the tested groups (P-value = 0.0014). Error bars represent SD.

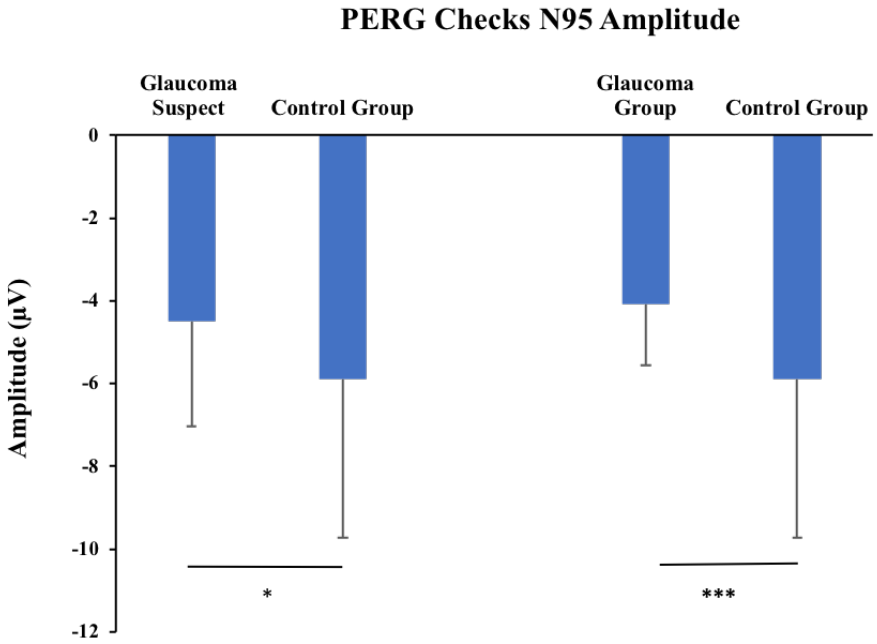

Figure 13: Comparison of PERG checks N95 amplitude between glaucoma and the control groups

Fisher's post-hoc analysis revealed that PERG checks N95 amplitude changes for both glaucoma suspect and glaucoma groups were statistically reduced compared to the control group. Error bars represent SD. * = P-value < 0.05, *** = P-value < 0.001.

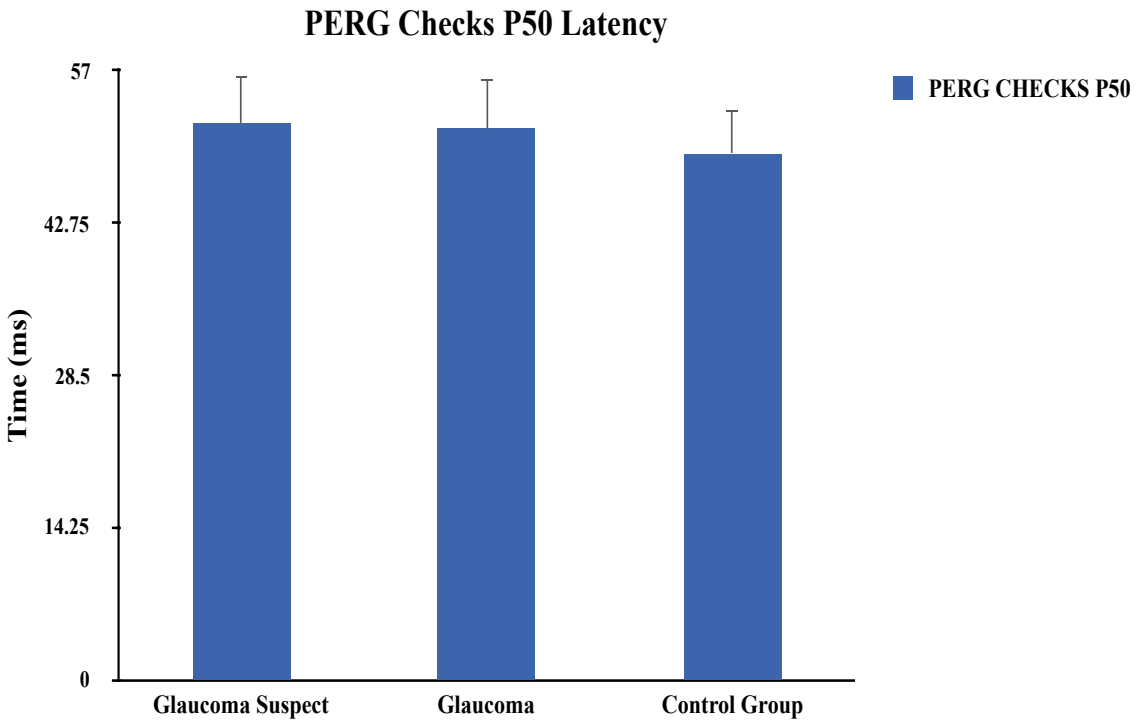

Figure 14: PERG checks P50 latency in the glaucoma groups and the control group

ANOVA revealed statistically significant results in the latency of the P50 component for PERG checks between the tested groups (P-value = 0.0009). Error bars represent SD.

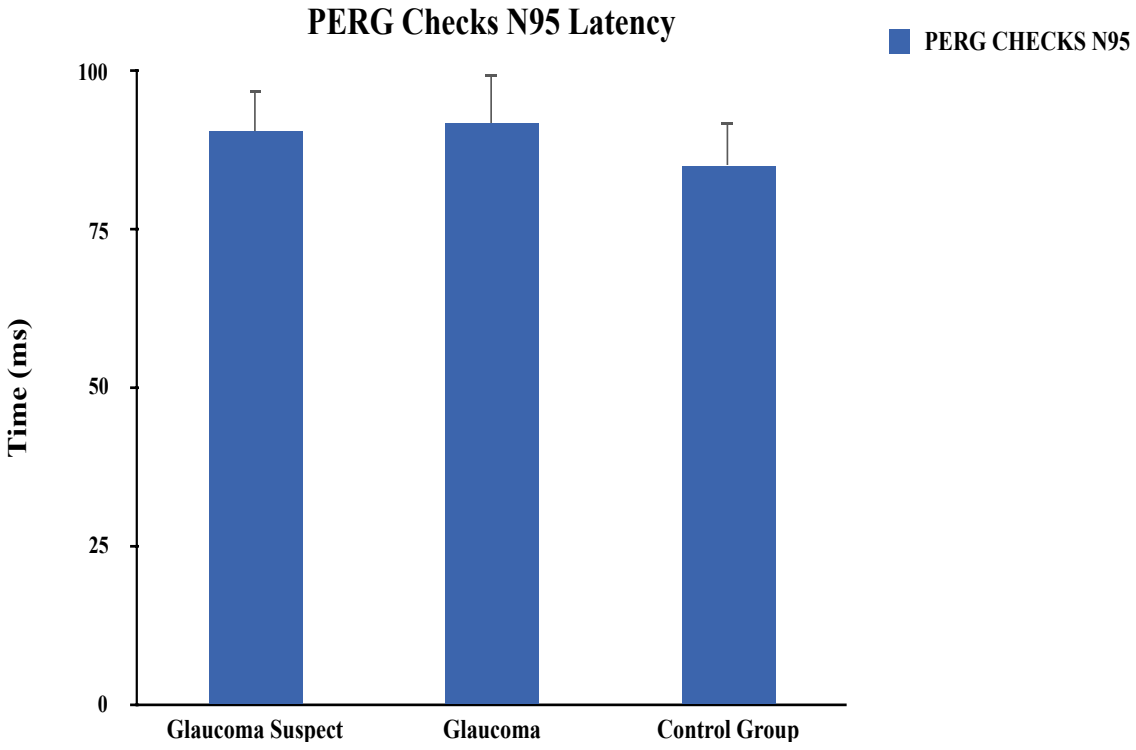

Figure 15: PERG checks N95 latency in the glaucoma groups and the control group.

ANOVA revealed a statistically significant difference (P-value < 0.0001) in the latency of PERG checks N95 between the examined groups. Error bars represent SD.

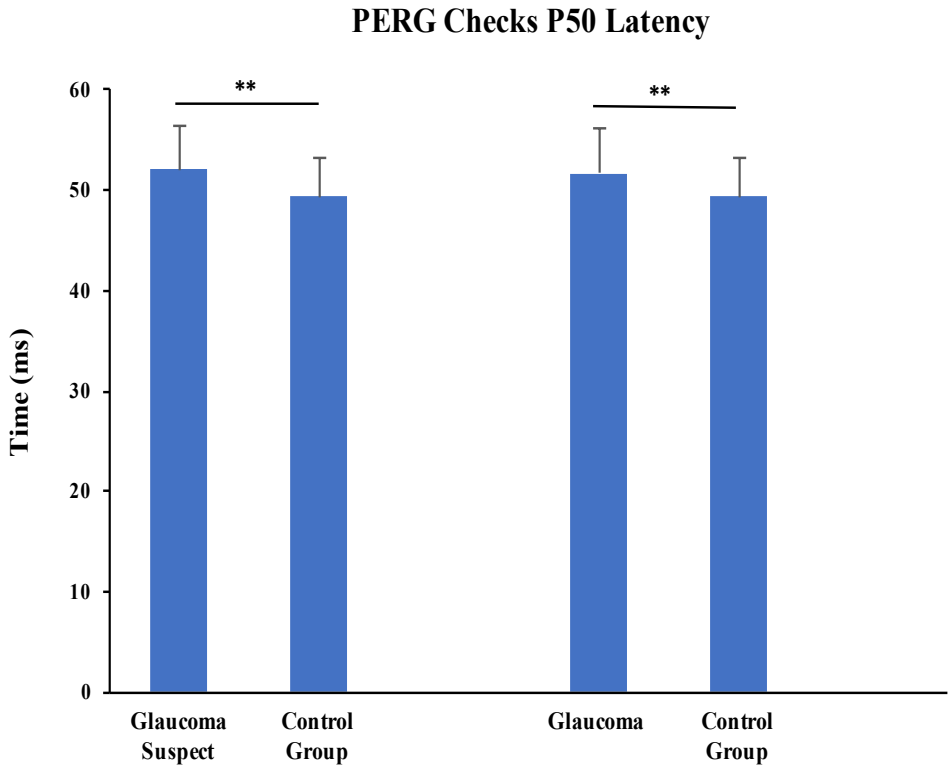

Figure 16: Comparison of PERG checks P50 latency between glaucoma and the control groups

Fisher's post-hoc analysis revealed that PERG checks P50 latency for both glaucoma suspect and glaucoma groups was significantly delayed in comparison to the control group. Error bars represent SD. ** = P-value < 0.01.

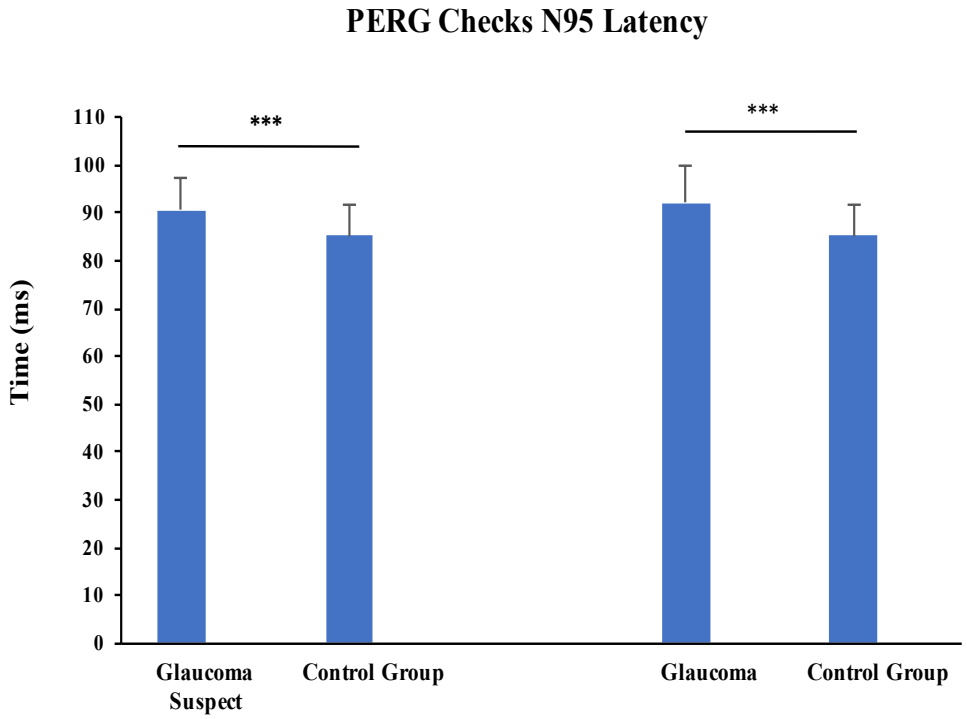

Figure 17: Comparison of PERG checks N95 latency between glaucoma and the control groups

PERG checks N95 latency for each group was statistically delayed compared to the control group. Error bars represent SD. *** = P-value < 0.001.

3.1.2. PERG bars N95 amplitude and latency detect changes in glaucoma patients

Next, we investigated whether PERG bars components were being affected by glaucoma. In the same patients as tested above, there was a trend towards a lower amplitude for P50; however, the trend did not reach significance (Figure 18). A decrease in N95 amplitude was observed in the tested groups by ANOVA with statistically significant results (P-value = 0.0005) (Figure 19). Also, a statistically significant decrease in the amplitude was documented by Fisher's post-hoc analysis for the N95 amplitude with glaucoma suspect and control groups (P-value = 0.0031) and glaucoma and control groups (P-value = 0.0004) (Figure 20).

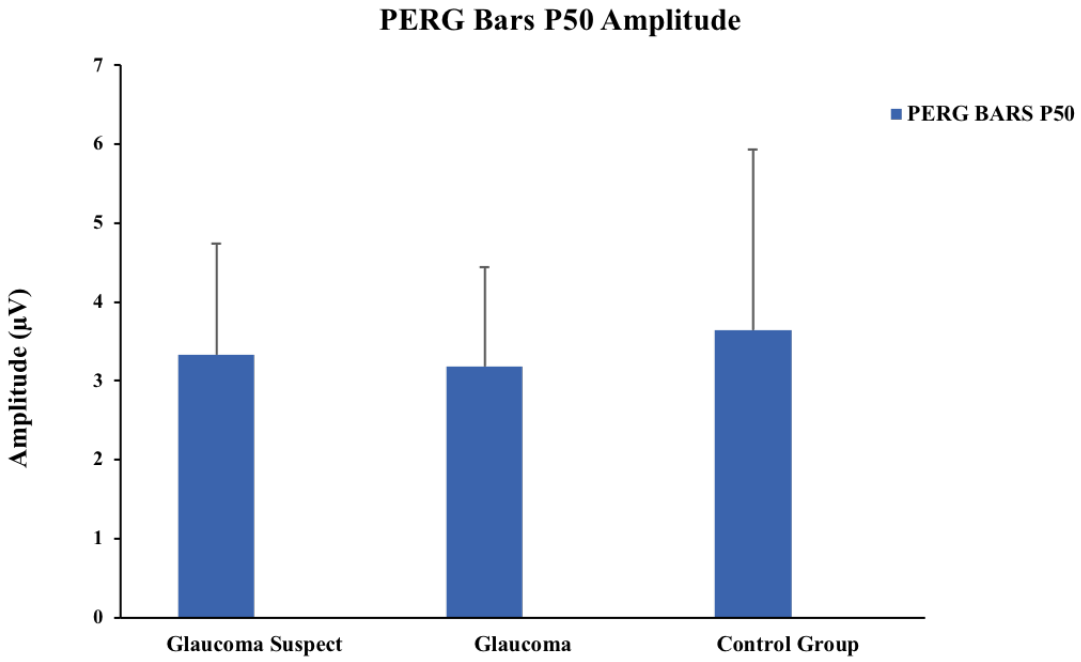

Figure 18: PERG bars P50 amplitude in the glaucoma groups and the control group

ANOVA revealed that PERG bars P50 amplitude showed a trend towards lower values in the tested groups, but this trend did not reach significance. Error bars represent SD.

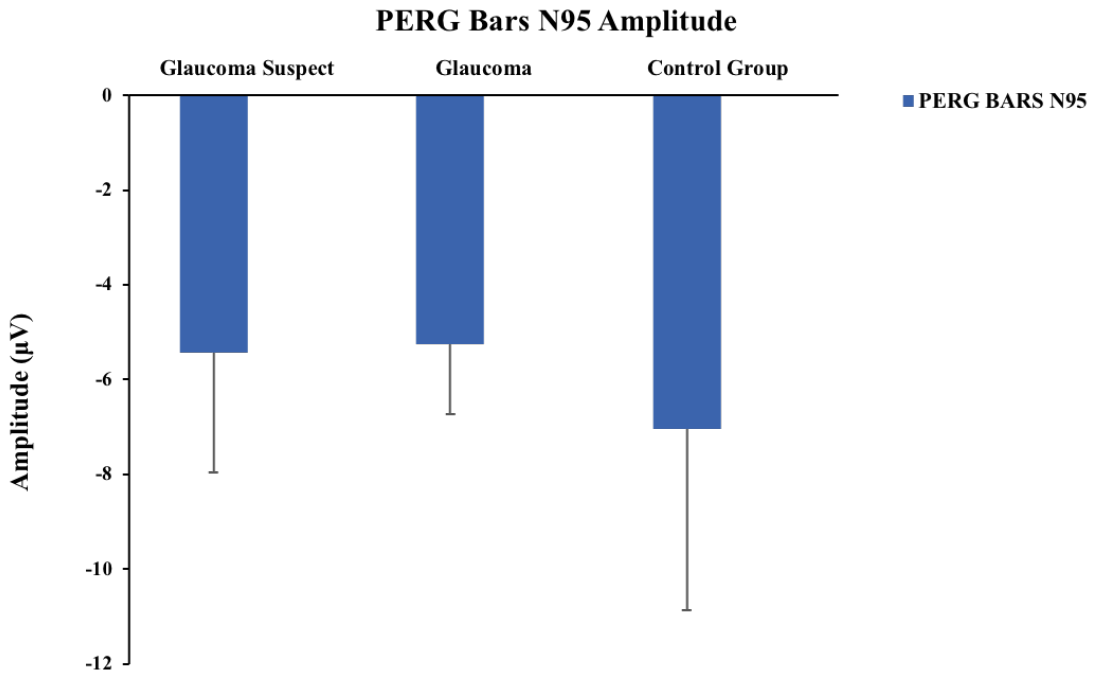

Figure 19: PERG bars N95 amplitude in the glaucoma groups and the control group

ANOVA revealed a statistically significant difference between groups in the N95 amplitude for PERG bars stimulus (P-value = 0.0005). Error bars represent SD.

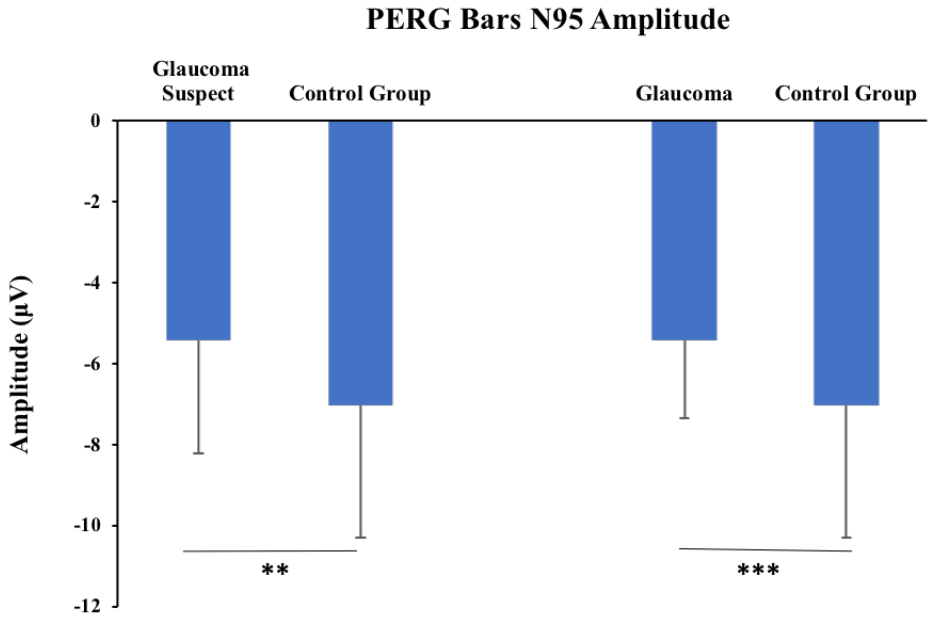

Figure 20: Comparison of PERG bars N95 amplitude between glaucoma and the control groups

Statistically significant results were detected by Fisher's post-hoc analysis in both glaucoma suspect and glaucoma groups compared to the control group. Error bars represent SD. ** = P-value < 0.01, *** = P-value < 0.001.

For the PERG bars test, ANOVA revealed a significant difference between experimental groups for the latencies of both the P50 and N95 components (P-value = 0.0053, and P-value < 0.0001, respectively). (Figures 21,22). However, when each of the components was examined separately by Fisher's post-hoc analysis, it was shown that the P50 component only showed a statistically significant longer latency between glaucoma and control groups (P-value = 0.0012) (Figure 23), whereas, with N95 latency data, statistically significant results were recorded between glaucoma suspect and control groups (P-value = 0.0007), and glaucoma and control groups (P-value < 0.0001) (Figure 24).

Altogether, these results suggest that PERG bars N95 amplitude and latency can detect changes related to glaucoma with a significant difference between glaucoma and glaucoma suspect groups and the control group. However, PERG bars P50 latency was able to identify changes only between the glaucoma groups and the control group. The amplitude and the latency values for both PERG P50 and N95 checks and bars is summarized in Table 1.

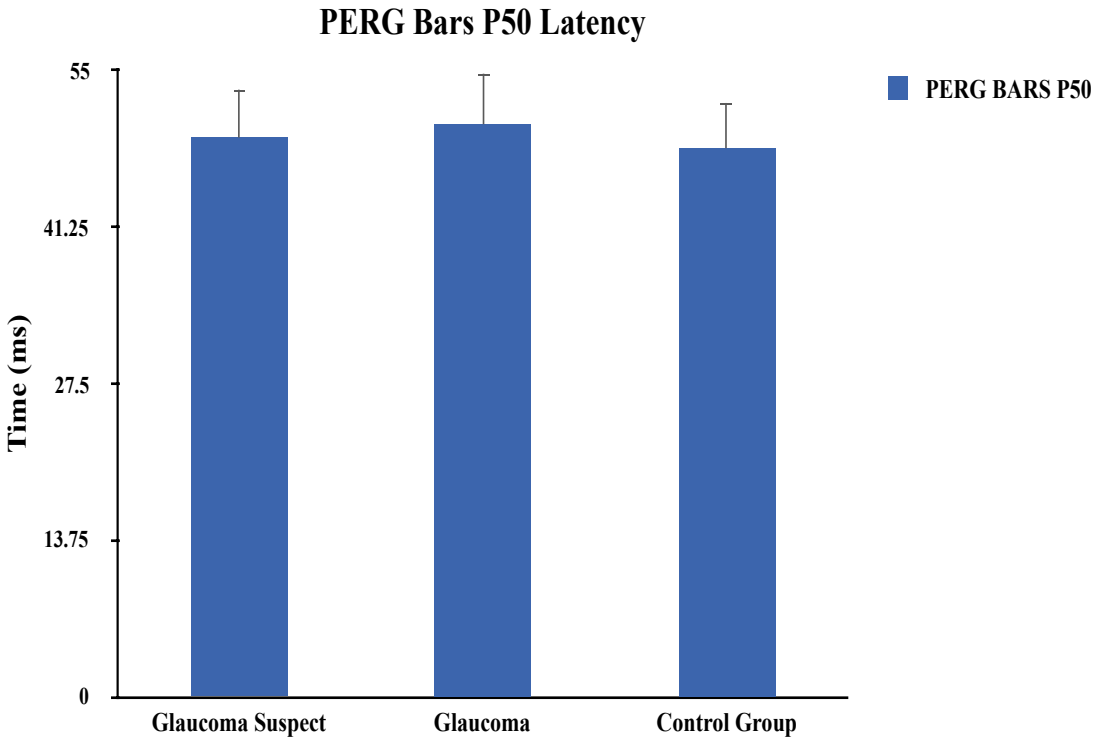

Figure 21: PERG bars P50 latency in the glaucoma groups and the control group

ANOVA revealed statistically significant (P-value = 0.0053) differences between the experimental groups. Error bars represent SD.

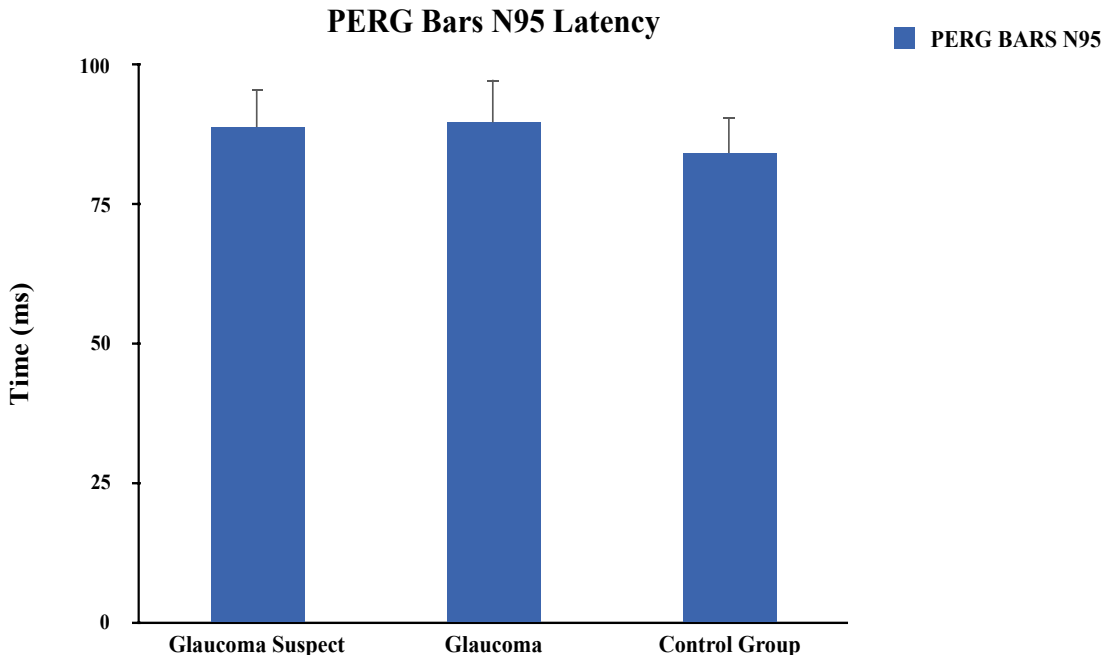

Figure 22: PERG bars N95 latency in the glaucoma groups and the control group

The latency of PERG bars N95 was delayed in the examined groups, and ANOVA revealed a statistically significant result (P-value < 0.0001). Error bars represent SD.

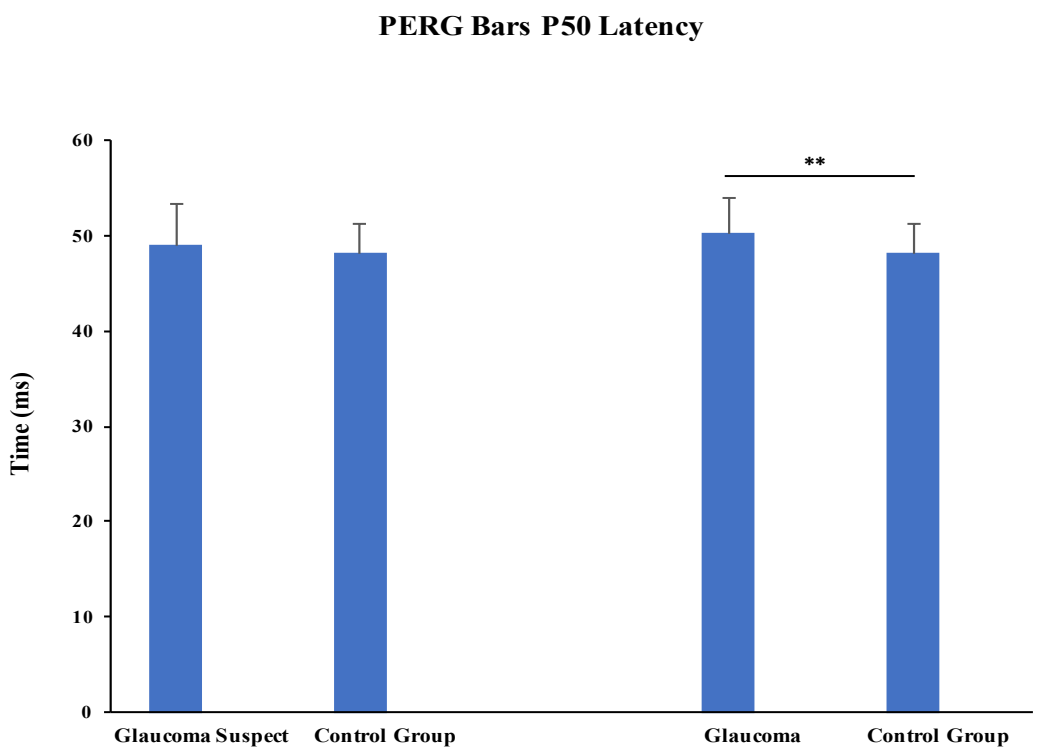

Figure 23: Comparison of PERG bars P50 latency between glaucoma and the control groups

The PERG bars P50 latency detected significant changes between the glaucoma and the control groups, but no significant change was detected between glaucoma suspect and the control groups. Error bars represent SD. ** = P-value < 0.01.

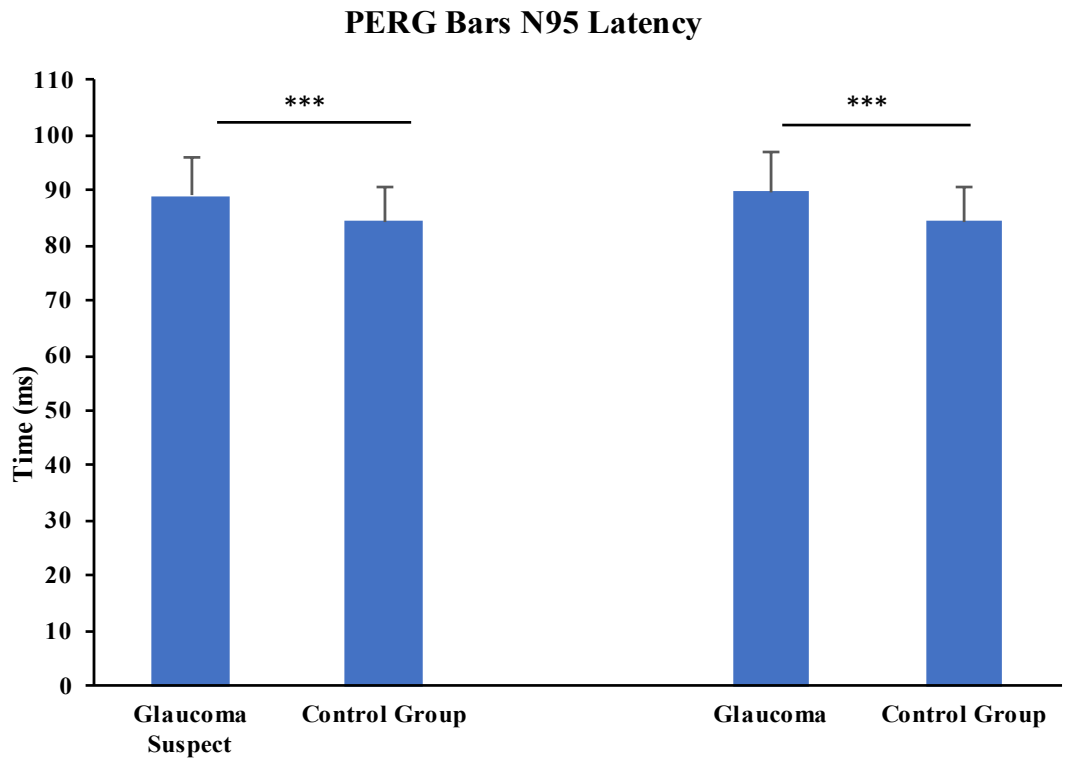

Figure 24: Comparison of PERG bars N95 latency between the control and the glaucoma groups

The PERG bars N95 latency detected changes between the control and each of the glaucoma groups. Error bars represent SD, *** = P-value < 0.001.

Test	ANOVA	Glaucoma suspect and glaucoma groups	Glaucoma suspect and control groups	Glaucoma and control groups
PERG checks P50 amplitude	N/S	N/S	N/S	N/S
PERG checks N95 amplitude	0.0014	N/S	0.0128 (*)	0.0006 (***)
PERG checks P50 latency	0.0009	N/S	0.0012 (**)	0.0020 (**)
PERG checks N95 latency	< 0.0001	N/S	0.0001 (***)	<0.0001 (***)
PERG bars P50 amplitude	N/S	N/S	N/S	N/S
PERG barsN95 amplitude	0.0005	N/S	0.0031 (**)	0.0004 (***)
PERG bars P50 latency	0.0053	N/S	N/S	0.0012 (**)
PERG bars N95 latency	< 0.0001	N/S	0.0007 (***)	< 0.0001 (***)

Table 1: The amplitude and the latency of PERG P50 and N95 checks and bars

A summarized table of the amplitude and the latency values for PERG checks and bars P50 and N95 components.

3.1.3. High specificity for PERG checks and bars N95 amplitude and latency

The sensitivity of a test is its ability to correctly identify patients that have the disease based on a gold standard test for the diagnosis (in this case SAP). The specificity is the ability to identify patients that do not have the disease. The sensitivity and specificity were calculated using the two by two (2 X 2) table with cutoff values of two standard deviations from the mean value for both PERG parameters, while mean deviation (MD) was -6 dB based on the Canadian Glaucoma Guidelines for classifying glaucoma stages (Rafuse and Buys, 2009).

In general, the specificity results were higher than sensitivity results for both PERG check and bars N95 for amplitude and latency. PERG checks N95 amplitude showed a sensitivity of 60% (i.e., it gave a positive result for 3 of 5 confirmed glaucoma cases), and a specificity of 89.18% (Table 1). N95 latency values showed 80% for sensitivity and 91.6% for specificity (Table 2). For PERG bars N95 amplitude sensitivity was 66.6%, and specificity was 83.8% (Table 3). The sensitivity of PERG bars N95 latency was 60%, and the specificity was 97.8% (Table 4). The sensitivity and specificity values for PERG N95 checks and bars are summarized in Table 5. Overall, our results revealed that PERG N95 checks and bars amplitude and latency were able to identify patients without glaucomatous changes.

N95 cutoff < 2.1 μV
MD cutoff < -6 dB

		Reference test SAP (MD)	
		Positive	Negative
Target test N95 PERG checks amplitude	Positive	3 (TP)	4 (FP)
	Negative	2 (FN)	33 (TN)
	Total	5	37

Sensitivity = 3/5 = 60%
Specificity = 33/37 = 89.18%

Table 2: Sensitivity and specificity of PERG checks N95 amplitude

The table shows the cutoff values for N95 and MD with sensitivity and specificity results based on the results of both PERG checks N95 amplitude and SAP (Measured in MD).

N95 cutoff > 98.7 ms
MD cutoff < -6 dB

		Reference test SAP (MD)	
		Positive	Negative
Target test N95 PERG checks latency	Positive	8 (TP)	3 (FP)
	Negative	2 (FN)	33 (TN)
	Total	10	36

Sensitivity = 8/10 = 80%
Specificity = 33/36 = 91.6%

Table 3: Sensitivity and specificity of PERG checks N95 latency

The table shows the cutoff values for N95 and MD with sensitivity and specificity results based on the results of both PERG checks N95 latency and SAP (Measured in MD).

N95 cutoff < 3.77 μV
MD cutoff < -6 dB

		Reference test SAP (MD)	
		Positive	Negative
Target test N95 PERG bars amplitude	Positive	6 (TP)	5 (FP)
	Negative	3 (FN)	26 (TN)
	Total	9	31

Sensitivity = 6/9 = 66.6%
Specificity = 26/31 = 83.8%

Table 4: Sensitivity and specificity of PERG bars N95 amplitude

The table shows the cutoff values for N95 and MD with sensitivity and specificity results based on the results of both PERG bars N95 amplitude and SAP (Measured in MD).

N95 cutoff > 96.9 ms
MD cutoff < -6 dB

		Reference test SAP (MD)	
		Positive	Negative
Target test N95 PERG bars latency	Positive	6 (TP)	1 (FP)
	Negative	4 (FN)	46 (TN)
	Total	10	47

Sensitivity = 6/10 = 60%
Specificity = 46/47 = 97.8%

Table 5: Sensitivity and specificity of PERG bars N95 latency

The table shows the cutoff values for N95 and MD with sensitivity and specificity results based on the results of both PERG bars N95 latency and SAP (Measured in MD).

PERG parameters	Sensitivity %	Specificity %
PERG Checks N95 amplitude	60%	89.18%
PERG Checks N95 latency	80%	91.6%
PERG bars N95 amplitude	66.6%	83.8%
PERG bars N95 latency	60%	97.8%

Table 6: Sensitivity and specificity of PERG checks and bars for N95.

A summarized table of the sensitivity and specificity values for PERG checks and bars N95 components.

3.2. Uniform Field Electroretinogram

3.2.1. Statistically significant decrease in PhNR amplitude in glaucoma groups

In order to understand the effect of glaucoma on UF-ERG components, the UF-ERG test was recorded in both glaucoma and control groups. The ANOVA results showed a trend towards lower amplitude for a-waves (Figure 25), but this did not reach statistical significance. The b-waves do not appear to be affected (Figure 26). This finding is consistent with the fact that the electrical activities within RGCs and optic nerve do not contribute to generating a- or b-waves. Therefore, glaucoma, which mostly affects RGCs does not diminish ERG a-wave or b-wave amplitudes (Fishman, 1985; Viswanathan et al., 1999). PhNR amplitude, on the other hand, was significantly decreased in the tested groups (P-value of 0.0002) (Figures 27). Notably, there were significant differences with Fisher's post-hoc analysis between glaucoma suspect and control groups (P-value of 0.0009) and the glaucoma group and control group (P-value of < 0.0001) (Figure 28).

3.2.2. Statistically significant delay in PhNR latency in glaucoma groups

The latency of a- and b-waves for glaucoma patients do not appear to be affected in the experimental groups (Figures 29, 30). However, ANOVA revealed that PhNR latency was significantly increased in the examined groups (P-value <0.0001) (Figure 31). A post-hoc analysis revealed significant differences between the glaucoma suspect group and the control group as well as the glaucoma group and the control group (P-value of <

0.0001; Figure 32). Overall, our data demonstrate that the UF-ERG PhNR amplitude and latency were able to detect glaucomatous changes in the glaucoma groups compared to the control group. The amplitude and the latency values for a-wave, b-wave, and PhNR is summarized in Table 7.

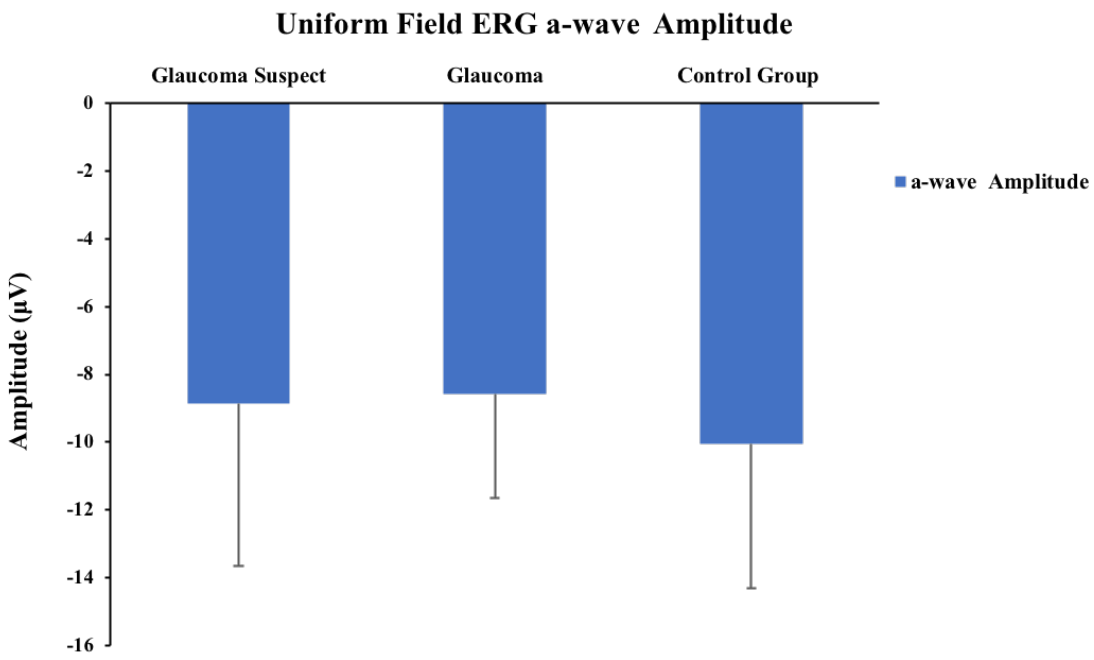

Figure 25: UF-ERG a-wave amplitude in the glaucoma groups and the control group

There appears to be a trend towards lower values in the a-wave in the examined groups, but ANOVA did not reveal statistically significant differences. Error bars represent SD.

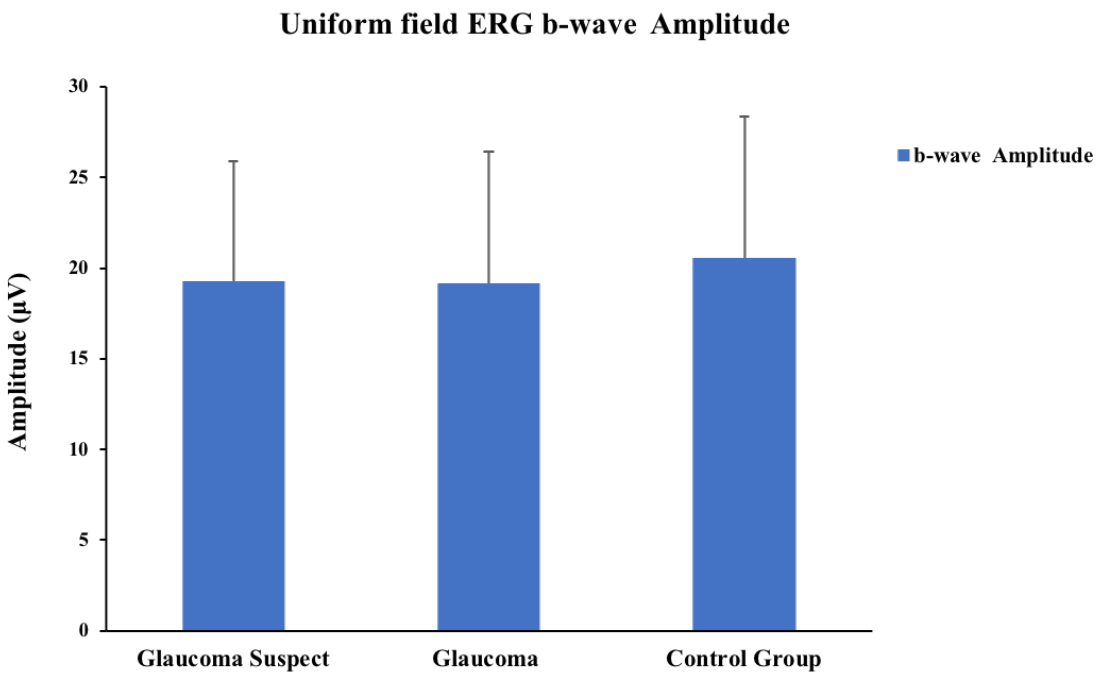

Figure 26: UF-ERG b-wave amplitude in the glaucoma groups and the control group

The amplitude of the b-wave does not appear to be affected in the examined groups by ANOVA. Error bars represent SD.

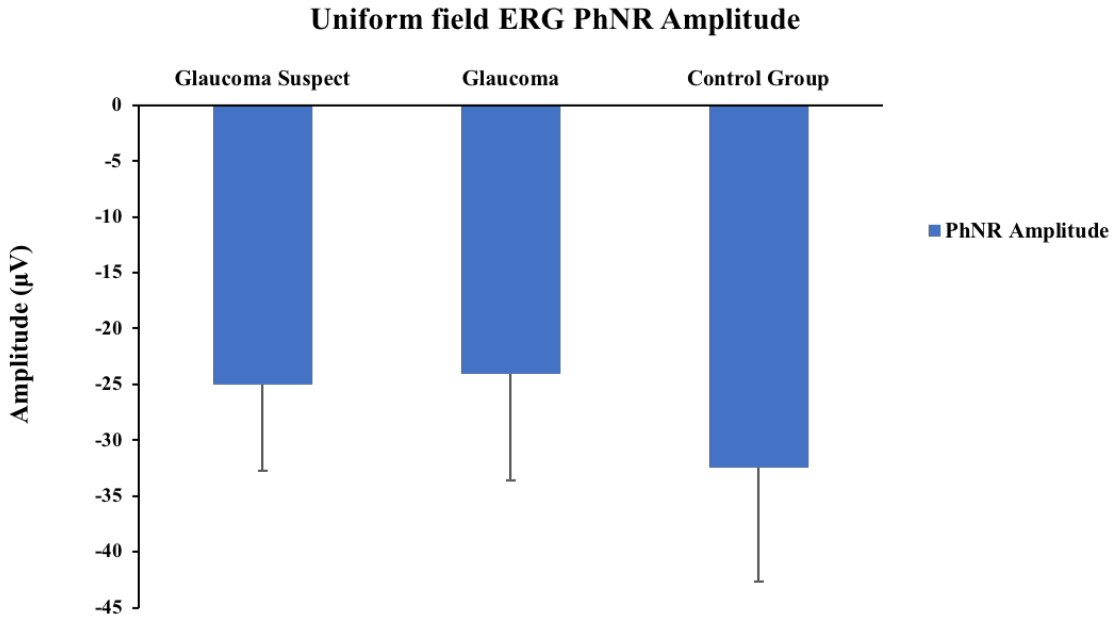

Figure 27: UF-ERG PhNR amplitude in the glaucoma group and the control group

ANOVA showed a significant difference between the groups for the UF-ERG PhNR amplitude (P-value = 0.0002). Error bars represent SD.

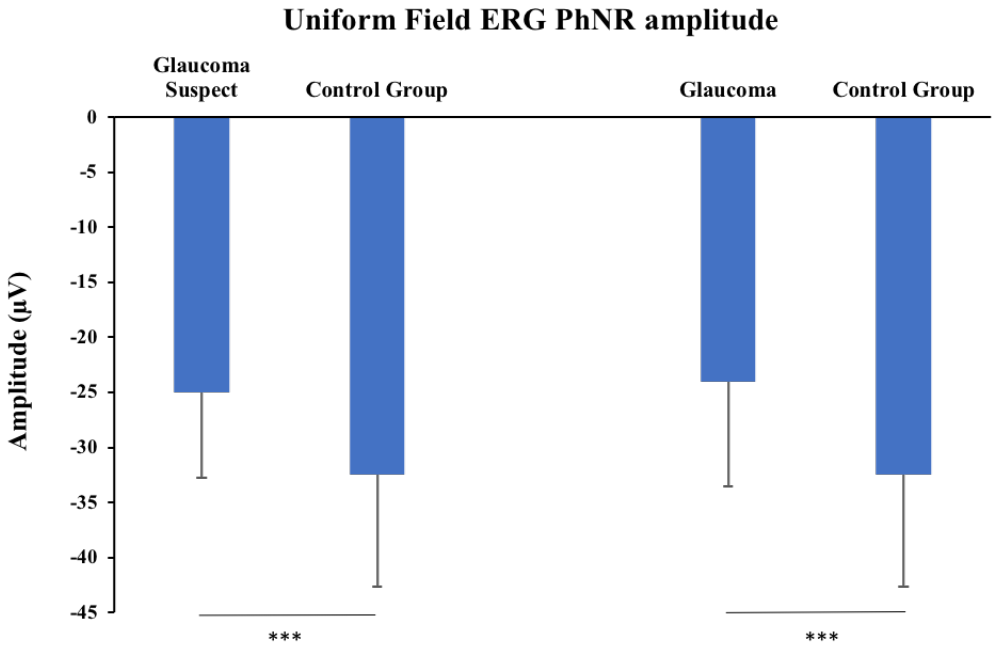

Figure 28: Comparison of PhNR amplitude between glaucoma and the control groups

Fisher's Post-hoc analysis showed a significant reduction in UF-ERG PhNR amplitude between the glaucoma group and the control group and between the glaucoma suspect group and the control group. Error bars represent SD. *** = P-value < 0.001.

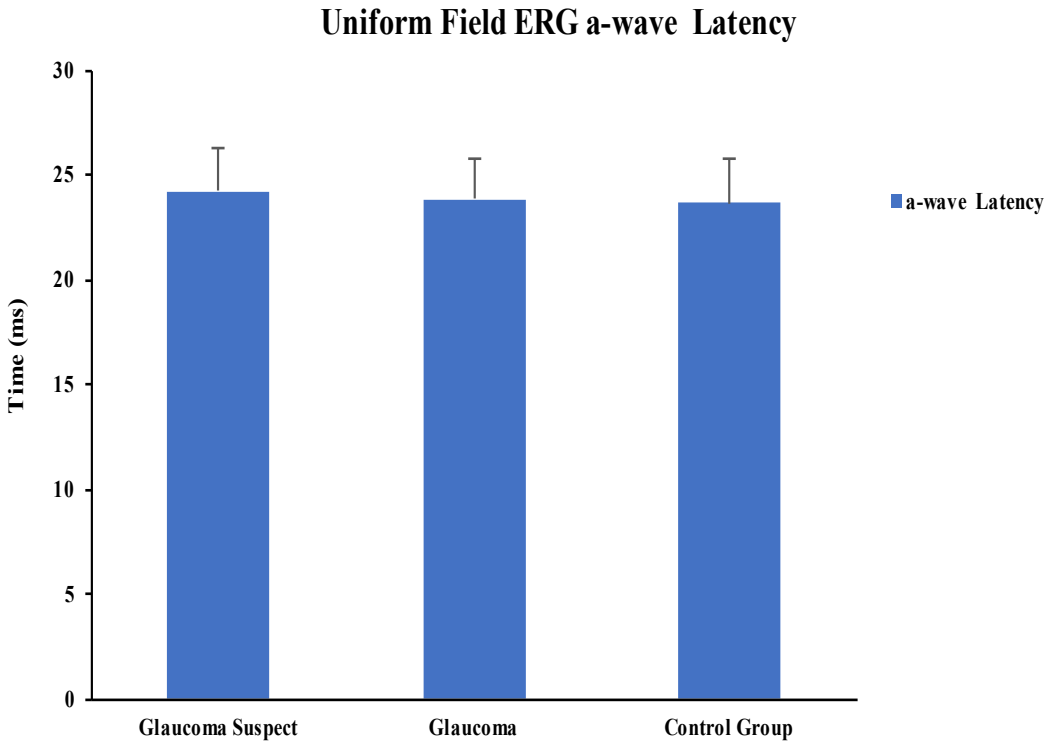

Figure 29: UF-ERG a-wave latency in the glaucoma groups and the control group

The latency of the a-wave does not appear to be different between the examined groups by ANOVA. Error bars represent SD.

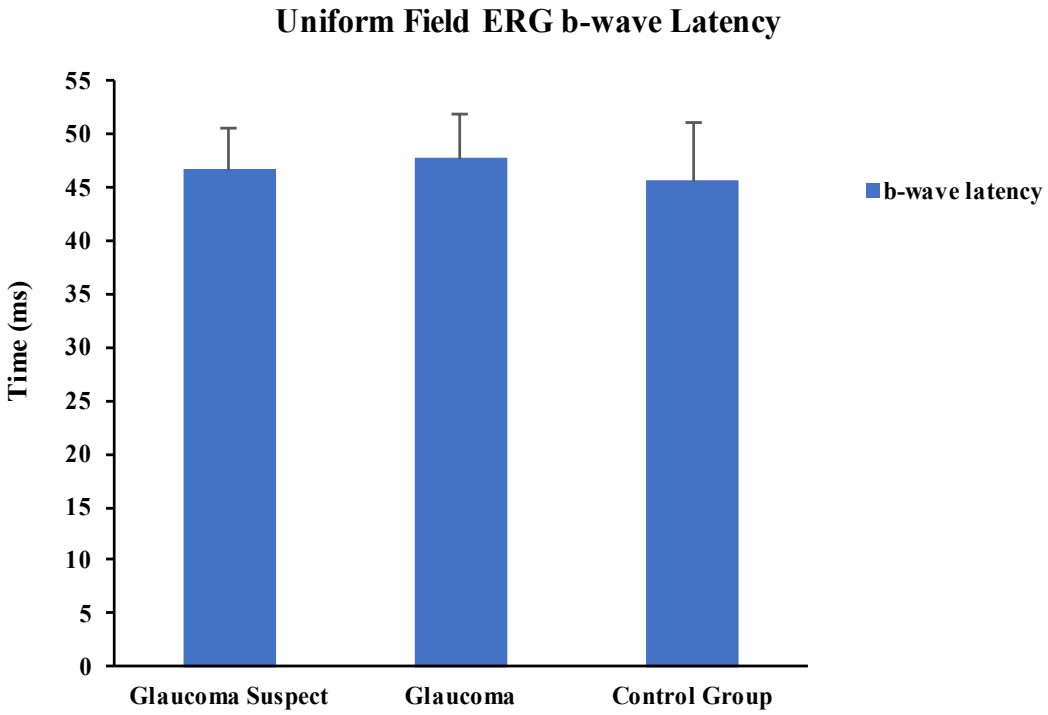

Figure 30: UF-ERG b-wave latency in the glaucoma groups and the control group

The latency of the b-wave does not appear to be affected in the tested patients by ANOVA. Error bars represent SD.

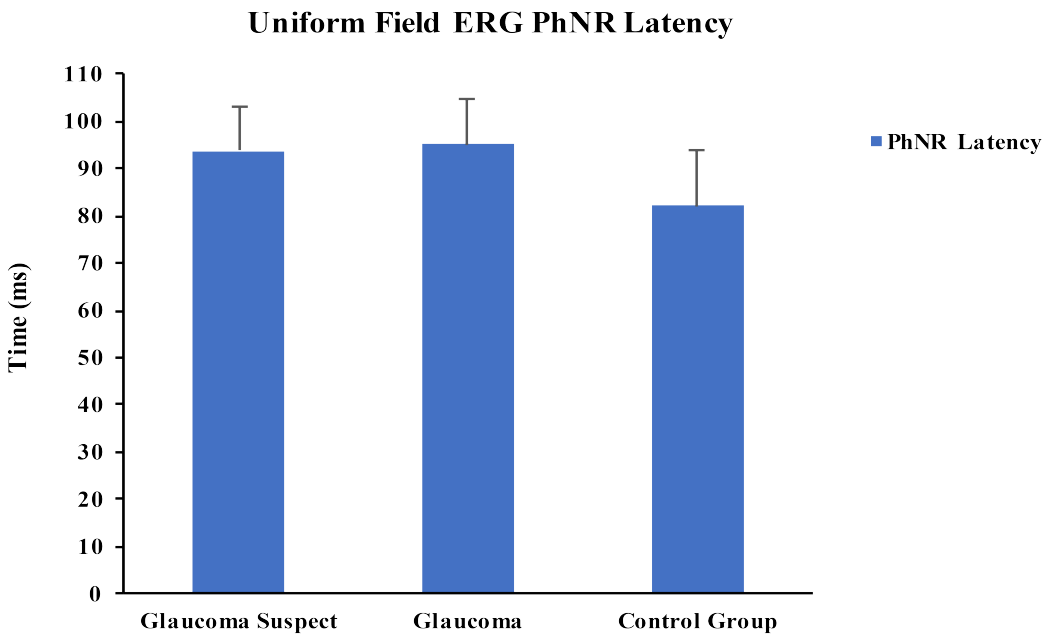

Figure 31: UF-ERG PhNR latency in the glaucoma groups and the control group

ANOVA revealed a significant difference between experimental groups for the latency of the PhNR (P-value < 0.0001). Error bars represent SD.

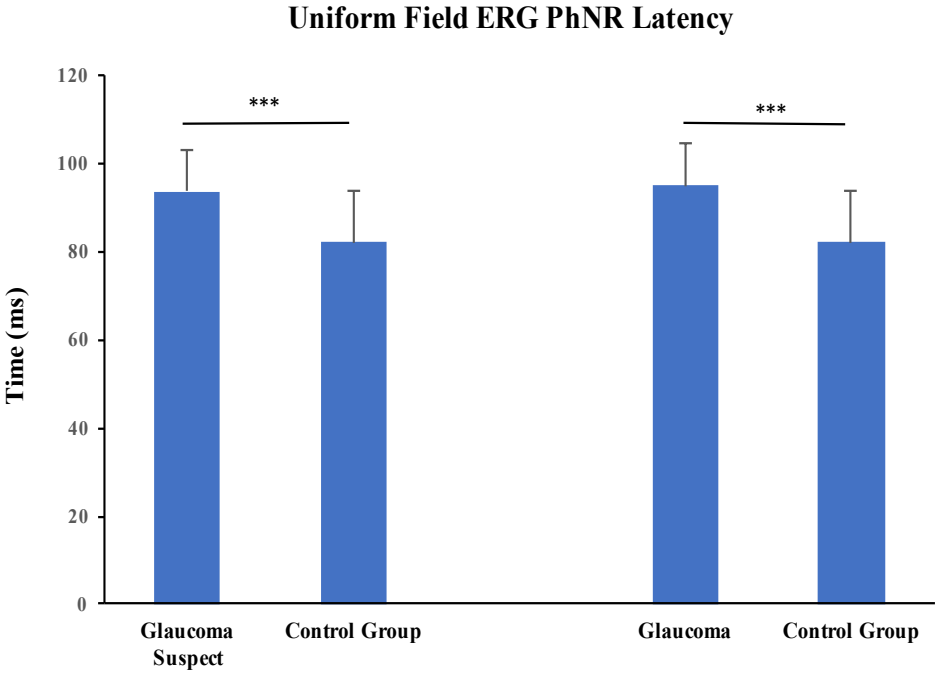

Figure 32: UF-ERG PhNR latency between the glaucoma groups and the control group

Fisher's post-hoc analysis detected UF-ERG PhNR prolonged latency between the glaucoma suspect group and the control group and between the glaucoma group and the control group. Error bars represent SD. *** = P-value < 0.001.

Test	ANOVA	Glaucoma suspect and glaucoma groups	Glaucoma suspect and control groups	Glaucoma and control groups
UF-ERG a-wave amplitude	N/S	N/S	N/S	N/S
UF-ERG b-wave amplitude	N/S	N/S	N/S	N/S
UF-ERG PhNR amplitude	0.0002	N/S	0.0009 (***)	< 0.0001 (***)
UF-ERG a-wave latency	N/S	N/S	N/S	N/S
UF-ERG b-wave latency	N/S	N/S	N/S	N/S
UF-ERG PhNR latency	< 0.0001	N/S	< 0.0001 (***)	< 0.0001 (***)

Table 7: The amplitude and the latency of UF-ERG components

A summarized table of the amplitude and the latency values for UF-ERG components.

3.2.3. High sensitivity for PhNR amplitude and high specificity for PhNR latency

PhNR amplitude showed a sensitivity of 83.3% and a specificity of 69.7% (Table 8), while latency values were 62.5% for sensitivity and 96.7% for specificity (Table 9). Overall, our results demonstrated that PhNR amplitude was able to identify patients with glaucomatous changes and the PhNR time component had the ability to identify patients without glaucomatous changes. Sensitivity and specificity values for PhNR amplitude and latency are summarized in Table 10.

PhNR cutoff < 22.2 μV
MD cutoff < -6 dB

		Reference test SAP (MD)	
		Positive	Negative
Target test PhNR amplitude	Positive	5 (TP)	13 (FP)
	Negative	1 (FN)	30 (TN)
	Total	6	43

Sensitivity = 5/6 = 83.3%
Specificity = 30/43 = 69.7%

Table 8: Sensitivity and specificity of PhNR amplitude

The table shows the cutoff values for PhNR amplitude and mean deviation (MD) with sensitivity and specificity results based on the results of both PhNR amplitude and SAP (Measured in MD).

PhNR cutoff > 106 ms
MD cutoff < -6 dB

		Reference test SAP (MD)	
		Positive	Negative
Target test PhNR latency	Positive	5 (TP)	1 (FP)
	Negative	3 (FN)	30 (TN)
	Total	8	31

Sensitivity = 5/8 = 62.5%
Specificity = 30/31 = 96.7%

Table 9: Sensitivity and specificity of PhNR latency

The table shows the cutoff values for PhNR latency and MD with sensitivity and specificity results based on the results of both PhNR latency and SAP (Measured in MD).

UF-ERG parameters	Sensitivity %	Specificity %
PhNR amplitude	83.3%	69.7%
PhNR latency	62.5%	96.7%

Table 10: Sensitivity and specificity of PhNR amplitude and latency

A summary table of the sensitivity and specificity values for PhNR amplitude and latency.

3.3. Comparison between PERG checks and bars N95 and PhNR parameters

3.3.1. PhNR can detect early glaucomatous changes

Since PERG N95 (for both checks and bars) and PhNR reflect RGC activities (Lam, 2005; Viswanathan et al., 2000), and we show above that both amplitude and latency of these tests are affected in glaucoma groups, we compared their effects side-by-side in order to determine if one test is better at detecting glaucomatous changes relative to the others. The result of comparing the amplitude of PERG checks and bars for N95 and PhNR demonstrated that all the tests detected a low amplitude for glaucoma groups (Figure 33).

PhNR was more sensitive in detecting glaucomatous changes in glaucoma suspect patients compared to PERG checks and bars stimuli (as shown by the lower P - value). PERG bars N95 had better ability in detecting glaucoma-related changes than PERG checks N95 in glaucoma suspect group. However, both PhNR and PERG checks and bars showed a similar ability to detect glaucomatous changes in the glaucoma group as is shown in Figure 33. Regarding the latency, PERG checks and bars N95 and PhNR recorded a delayed response as compared to the control group. A similar ability to detect glaucoma-related changes in the form of longer latency was observed in glaucoma suspect and glaucoma groups with both PhNR and PERG checks and bars N95 (Figure 34).

Overall, the data showed that PhNR is more sensitive in detecting glaucomatous changes in the glaucoma suspect group in terms of low amplitude compared to PERG checks and bars N95 (Figure 33). Based on prolonged latency, PhNR and PERG checks and bars N95 did not show any difference in their ability to detect glaucomatous changes in the glaucoma suspect as well as glaucoma groups (Figure 34).

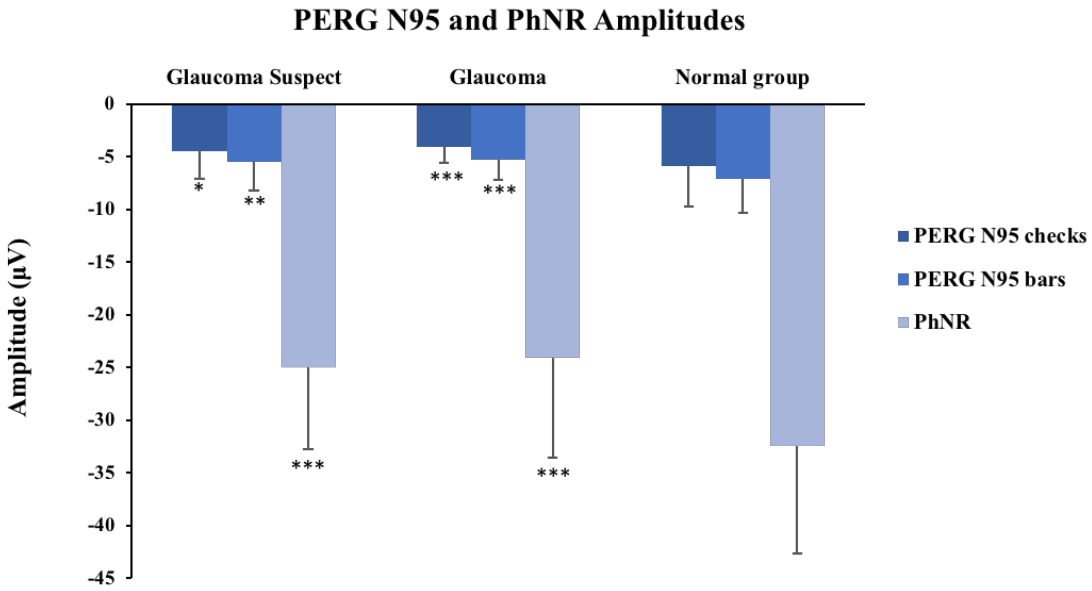

Figure 33: Comparison between PERG checks and bars N95 and PhNR amplitude

PERG checks and bars N95 and PhNR detected glaucomatous changes in terms of low amplitude. PhNR showed statistically significant results with higher P-values than the other tests in the glaucoma suspect group compared to the control group. Error bars represent SD. * = P-value < 0.05, ** = P-value < 0.01, *** = P-value < 0.001.

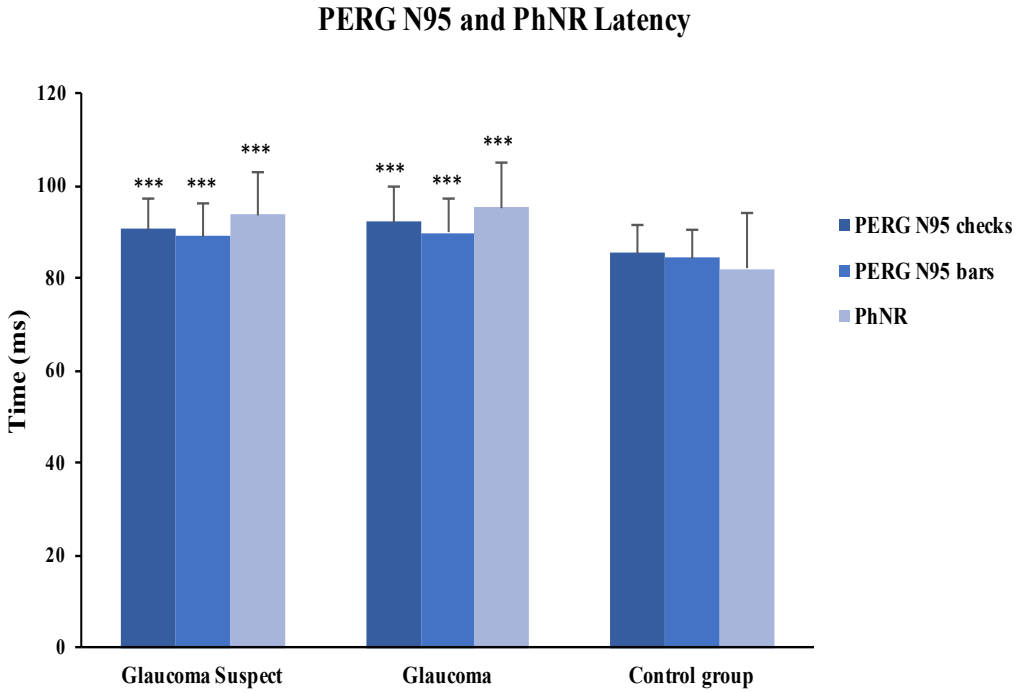

Figure 34: Comparison between PERG checks and bars N95 and PhNR latency

The latency of PERG checks and bars N95 and PhNR were delayed in the glaucoma groups with statistically significant results. Error bars represent SD. *** = P-value < 0.001.

3.4. Visual field mean deviation changes with glaucoma groups

Visual field (VF) assessment is one of the standard diagnostic methods which is used by clinicians in diagnosing and monitoring glaucomatous changes (Miglior et al., 1996). Fisher's post-hoc results demonstrated that a statistically significant decline in MD was identified by SAP between glaucoma suspect and glaucoma groups (P-value = 0.0370) (Figure 35).

3.5. Retinal nerve fiber layer thinning is seen in glaucoma groups

Optical coherence tomography (OCT) provides quantitative data for the clinicians through RNFL assessment. It is believed that OCT can detect glaucomatous retinal changes before any VF defects can be identified by SAP (Sharma et al., 2008). Based on our findings, a statistically significant decrease in RNFL thickness was identified by OCT, specifically between glaucoma suspect and glaucoma patients (P-value = 0.0007) (Figure 36).

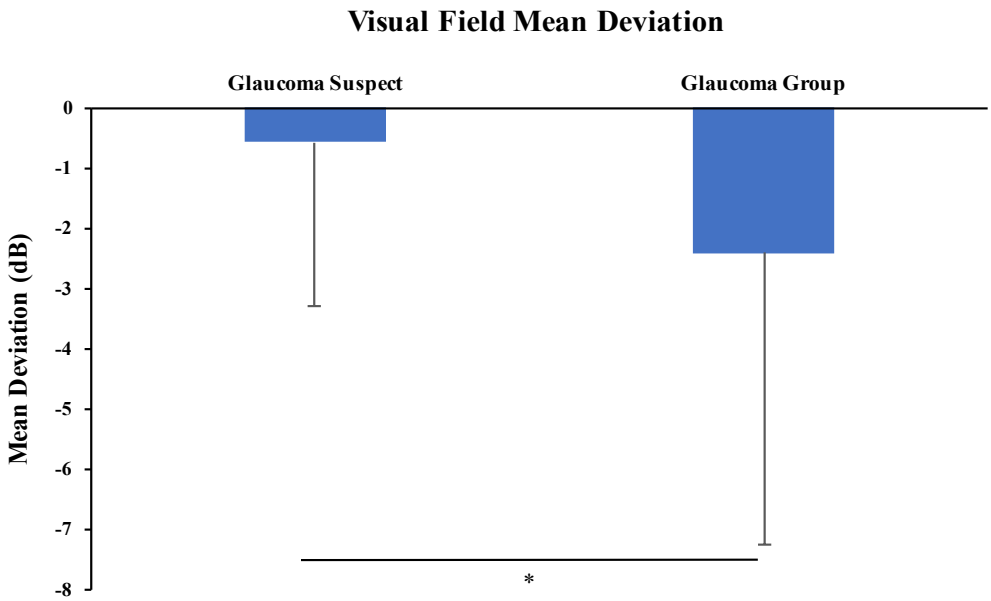

Figure 35: Visual field mean deviation between the glaucoma groups

Visual field mean deviation value was statistically significant between glaucoma groups (P-Value 0.0370). Error bars represent SD. * = P-value < 0.05.

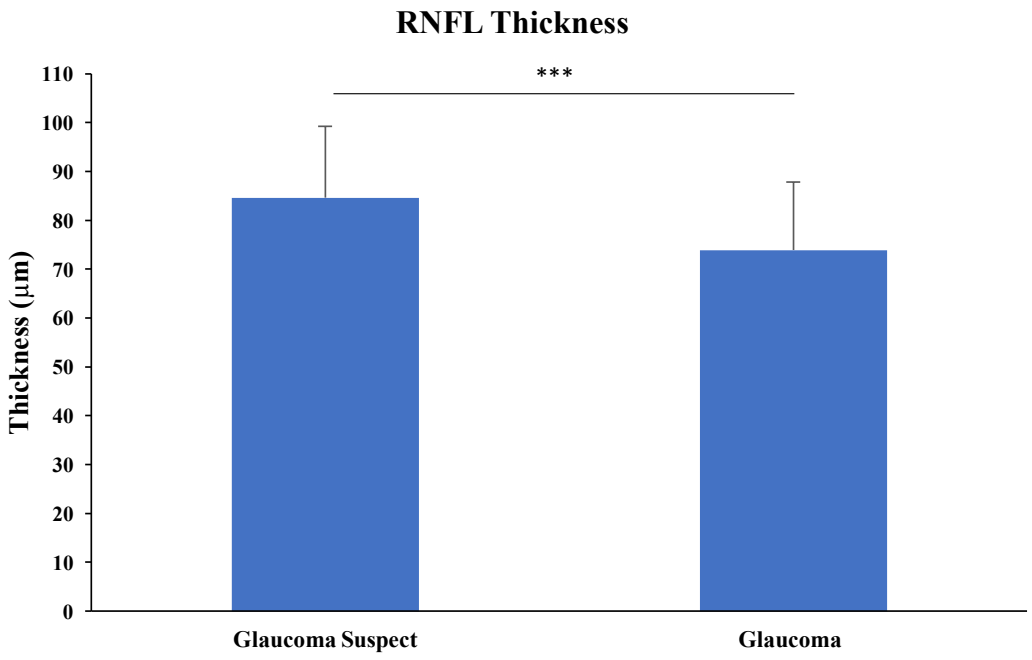

Figure 36: Retinal nerve fiber layer thickness between the glaucoma groups

The RNFL thickness readings were statistically significant between glaucoma groups (P-Value = 0.0007). Error bars represent SD. *** = P-value < 0.001.

4-Discussion

In our study, the effects of glaucomatous changes on both PERG checks and bars and UF-ERG components were explored in terms of amplitude and latency. For the first time, we used the Diagnosys D-341 Attaché-Envoy Electrophysiology System to record both PERG checks and bars stimulation as well as UF-ERG in glaucoma suspect, glaucoma and control groups to detect glaucoma-related changes.

Our findings showed that the PERG checks and bars N95 component showed significant changes in terms of lower amplitude and longer latency in the glaucoma suspect and glaucoma groups relative to the control group. However, the P50 component for PERG checks and bars showed only significantly longer latency. Regarding the UF-ERG test, PhNR showed a significant decrease in the amplitude and longer latency for the glaucoma suspect and glaucoma groups in comparison to the control. With regards to sensitivity and specificity, both PERG checks and bars N95 revealed a similar ability to recognize individuals without glaucomatous changes with both amplitude and latency parameters (i.e., had high specificity). On the other hand, PhNR was able to identify people with or without glaucomatous changes in the form of high amplitude sensitivity and high latency specificity. Notably, both PERG bars N95 and PhNR latency specificity (97.8% and 96.7% respectively) had the same potential to recognize individuals without glaucoma-related changes.

4.1. Pattern Electroretinography

4.1.1. Non-significant low amplitude trends and a significantly longer latency for PERG checks and bars P50

Objective assessment of RGC function can be achieved by using PERG. RGC function assessment can be carried out by evaluating PERG components, namely P50 and N95 (Holder, 2001). The effect of glaucoma on PERG components has been explored for many decades. Furthermore, PERG is considered as a crucial tool to evaluate RGC function in glaucoma (Bach et al., 2013; Bowd et al., 2009a; Fredette et al., 2008; Kreuz et al., 2014; Porciatti and Ventura, 2004; Ventura et al., 2013; Yang and Swanson, 2007). Extensive studies investigating glaucomatous changes have reported PERG amplitude reduction (Kreuz et al., 2014) and this reduction is related to RGC loss and or diminished activity of remaining viable RGCs (Banitt et al., 2013; Fredette et al., 2008; Kreuz et al., 2014; Ventura et al., 2013).

Studies of PERG time components (latencies) in glaucoma have revealed delays in the response perhaps related to slower RGC responses to stimuli (Celesia et al., 1987; Kreuz et al., 2014; Porciatti and Ventura, 2004; Ventura et al., 2013). It is well known that in electrophysiology "the more pathologic, the slower" (Bach and Poloschek, 2013). It is believed that the ability of latency to detect glaucomatous changes in terms of longer latency compared to the amplitude is related to the variability in the nature of the amplitude compared to the latency. PERG amplitude is affected by different exogenous and

endogenous factors that do not have any influence on latency, namely the size of the pupil, the blood level of certain medications, diurnal variation, and others (Bearse et al., 2006; Jampol, 2001).

Our results revealed that the effect of glaucoma on PERG checks and bars showed a non-significant decrease in P50 amplitude. Non-significant P50 amplitude reduction might be related to the origin of the P50 waveform as it reflects RGC activities and other retinal cells (Holder, 2001; Viswanathan et al., 2000). Since glaucoma is a disease of exclusively RGCs, it might not be surprising that the P50 amplitude component, which is not solely RGC-derived, is not significantly affected. Our results are supported by a study that was done by Cvenkel et al., which also showed that the amplitude of PERG P50 did not show a significant decline in glaucoma patients or glaucoma suspects (Cvenkel et al., 2017). However, a significant decrease in P50 amplitude has been reported in both glaucoma and glaucoma suspects by other groups, which contradicts these findings (Ganekal et al., 2013; Neoh et al., 1994; O'Donaghue et al., 1992; Preiser et al., 2013).

Although, PERG time component has not been evaluated extensively (Bach and Poloschek, 2013; Bode et al., 2011; Kreuz et al., 2014; Ringens et al., 1986), a significant delay of P50 latency has been reported by Ganekal et al and Parisi et al. (Ganekal et al., 2013; Parisi et al., 2001). On the other hand, non-significant changes in the time component have been detected by Bode et al. and Ventura et al. on studies that were done on glaucoma patients (Bode et al., 2011; Ventura et al., 2005). Our study revealed a significant delay in

P50 latency for the PERG checks test for both glaucoma suspect and glaucoma groups compared to the control group. On the other hand, the P50 latency for the PERG bars test only identified a significant change in the glaucoma group in comparison to the control group.

The difference in our findings for PERG checks and bars P50 and N95 and some of the previous findings in the literature might be related to the use of different types of electrodes and recording protocols. On the other hand, the agreement between our study and some of those in the literature may reflect a similarity in recording protocols. Moreover, there are some variables that may affect the amplitude, such as dermal impedance and tear film resistance, which are not related to pathology per se. Consequently, the amplitude measures have higher variability than latency (Jampol, 2001).

Overall, our results for both PERG checks and bars showed that P50 amplitude was not a good measure of glaucomatous changes, and P50 latency was good at identifying early glaucoma changes in the PERG checks test but not in the PERG bars test. Therefore, going forward, we would suggest that the P50 component of the PERG is not ideal for early detection of glaucoma.

4.1.2. PERG N95 significantly affected in terms of low amplitude and longer latency

The retinal glaucomatous changes due to high IOP in terms of structure and function have been explored extensively in non-human primates as there are similarities in

ocular structure as well as visual function with humans (Glovinsky et al., 1991; Harwerth et al., 1997; Varma et al., 1992; Viswanathan et al., 1999). One study by Viswanathan et al. used tetrodotoxin (TTX) to block the spiking activity of both amacrine and RGCs (Viswanathan et al., 1999, 2001). The authors found that PERG changes due to experimental glaucoma were similar to intravitreal TTX effects on healthy non-human primate eyes. These findings suggest that the PERG response reduction is related to the deterioration of RGC spiking activity. Furthermore, Viswanathan et al. observed that N95 was reduced prominently with intravitreal TTX injection in non-human primates, whereas there was only a partial reduction in the P50 amplitude (Viswanathan et al., 2000).

Our results revealed that the N95 component for both PERG checks and bars showed a significant decrease in the amplitude and a prolonged latency for both the glaucoma suspect and glaucoma groups compared to the control group. Our findings are consistent with the results that have been reported by others (Bach and Hoffmann, 2008; Bach et al., 1988; Bode et al., 2011; Ganekal et al., 2013; Graham et al., 1996; Viswanathan et al., 2000). However, with glaucoma suspect patients, N95 amplitude did not show any significant decrease in a study that was done by Jafarzadehpour et al. (Jafarzadehpour et al., 2013). Their findings did not agree with our results or those reported by others (Bach and Hoffmann, 2008; Bach et al., 1988; Bode et al., 2011; Ganekal et al., 2013; Graham et al., 1996; Viswanathan et al., 2000),which showed a significant decline in N95 amplitude due to glaucomatous changes.

Regarding time component changes, PERG checks and bars N95 latency has shown a significant decrease in glaucoma suspects and glaucoma patients (Bach and Poloschek, 2013; Kreuz et al., 2014; Ringens et al., 1986), which is similar to the results of different studies that concluded a delay in N95 latency for both glaucoma suspect and early glaucoma patients (Jafarzadehpour et al., 2013; Kreuz et al., 2014). All these findings confirm our results in terms of a delayed N95 time component. On the other hand, the majority of early studies in glaucoma had previously reported non-significant changes in N95 latency (Bach and Hoffmann, 2008; van den Berg et al., 1986; Papst et al., 1984; Porciatti et al., 1987), which are in contrast to our findings in terms of a significant increase in latency. As it has mentioned previously in section 4.1.1, the reasons behind the similarity and discrepancy between our findings and other studies might be related to the electrode types and the recording protocol.

Unfortunately, there are a limited number of studies commenting on the effect of glaucoma on the time component (Kreuz et al., 2014), which is due to the difficulty of obtaining a consistent N95 latency estimate due to the broad N95 waveform (Bach et al., 2000; Holder, 2001). Therefore, time component assessment based on the ideal or smoothed waveform shape (Bach et al., 2013; Heckenlively and Arden, 2006) in addition to the amplitude, are essential since both of them reflect different aspects of RGC function (Jafarzadehpour et al., 2013) and are important elements in the PERG evaluation report. Furthermore, the ISCEV standards committee has recommended that the PERG report should comment on both amplitude and time components even with difficulty in obtaining N95 latency (Bach et al., 2000, 2013).

4.1.3. High specificity detected for both PERG checks and bars N95 amplitude and latency

In order to determine the validity of PERG, calculating the sensitivity and specificity would be the vital indicator for its efficacy in terms of detecting glaucomatous changes (Korth, 1997; Parikh et al., 2008). Our research has revealed that both PERG checks and bars N95 amplitude and latency have recorded high specificity. Sensitivity and specificity calculations for PERG checks N95 have been explored by O'Donaghue et al. and they have reported a sensitivity ranging from 75 - 94% for N95 amplitude, and specificity of 81 -100% (Korth, 1997; O'Donaghue et al., 1992). Also, Pfeiffer et al. have reported 82.7% sensitivity and 90.8% specificity for N95 amplitude (Ganekal et al., 2013; Pfeiffer and Bach, 1992). Our research findings are consistent with the previously mentioned results in terms of reporting high N95 amplitude specificity. Result consistency might be related to the similarity of the number of patients who were included in the sample size and the stage of glaucoma which was included in the tested sample. However, to our knowledge, sensitivity and specificity have not been calculated for PERG bars N95 amplitude. Also, the sensitivity and specificity of PERG checks and bars N95 latency have not been explored. Therefore, in the future, an extensive investigation should be carried out to determine PERG checks and bars' ability to differentiate between individuals with or without glaucoma. Altogether, PERG checks and bars N95 amplitude and latency showed the potential to identify candidates without glaucomatous changes.

4.1.4. Checks versus bars stimuli

PERG checks and bars component changes in the forms of lower amplitudes and delayed latency in glaucoma patients may be explained by RGC dysfunction due to glaucoma as it has been explored by many studies (Cvenkel et al., 2017; Viswanathan et al., 2000). The comparison of the two types of stimuli, namely checks and bars, has not been explored in the research field. Most studies have used either checks or bars stimuli to identify glaucoma-related changes (Bowd et al., 2009b, 2011; Cvenkel et al., 2017; Jafarzadehpour et al., 2013; Sehi et al., 2009; Ventura et al., 2005, 2013). ISCEV standards for PERG have focused mainly on PERG checks as a stimulus and stressed on the fact that any PERG stimulus shape, including bars, would not get different results if the stimulus parameters in the screen have met ISCEV recommendations (Bach et al., 2013).

As the Diagnosys D-341 Attaché-Envoy Electrophysiology System was recently introduced in the clinical setting, it is unknown whether PERG bars has the same ability as PERG checks to detect glaucoma-related changes in the form of low amplitude and longer latency. The data presented in this thesis represent the first findings on PERG checks vs. bars stimuli for glaucoma detection. Our results have concluded that both PERG N95 checks and bars amplitude and latency can detect glaucomatous changes. Specifically, the two tests have similar abilities in detecting glaucoma-related changes in glaucoma groups in the form of low amplitude and longer latency. Although both PERG checks and bars N95 have detected glaucoma-related changes in the glaucoma suspect group, the PERG bars stimulus is better than PERG checks N95 stimulus. In addition to that, both N95 PERG

checks and bars showed high specificity values which revealed a potential to be used as a diagnostic method for glaucoma detection. Based on these findings, adopting PERG bars as a diagnostic test would be beneficial as there are significant advantages to this stimulus over the check's stimulus. The difference in the recording time for PERG bars is one minute per eye compared to PERG checks which is three minutes per eye. Consequently, it might be practical to use PERG bars instead of PERG checks for glaucoma diagnosis. In future studies, it would be highly beneficial for researchers to investigate the potential use of PERG bars in glaucoma detection.

4.2. Uniform field electroretinography

4.2.1. UF-ERG PhNR shows glaucoma-related changes

Investigating UF-ERG waveform components origin opens the door for researchers to determine the possibility of using UF-ERG in glaucoma detection. Previous studies that looked at the origin of waveform components found that a- and b-waves reflect the activity of photoreceptors and bipolar cells, respectively (Brown and Watanabe, 1962; Heynen and van Norren, 1985; Sieving et al., 1994; Viswanathan et al., 2001; Whitten and Brown, 1973), whereas the PhNR response is generated by RGCs (Kinoshita et al., 2016; Viswanathan et al., 2000, 2001; Wilsey and Fortune, 2016). It has been shown that PhNR is generated by RGCs, which was provided by experiments in non-human primates that showed the intravitreal injection of TTX, which removes RGC spiking activity,

extinguished the PhNR (Kundra et al., 2016; Rangaswamy et al., 2004; Viswanathan et al., 1999, 2001). It is well known that glaucoma mainly affects RGCs and their axons and this appears as PhNR amplitude reduction. Moreover, as there is a similarity between PhNR that has been recorded from humans and non-human primates (Viswanathan et al., 1999), therefore, our results can be compared with research that has been carried out on non-human primates as well as humans.

Our study used the Diagnosys D-341 Attaché-Envoy Electrophysiology System to record UF-ERG and PERG on the same glaucoma groups and the control group at the same recording setting. We reported a significant decrease in PhNR amplitude and prolonged latency in glaucoma suspect and glaucoma groups compared to the control group. It has been documented that PhNR amplitude is reduced in three different glaucoma stages, namely early, moderate, and advanced, in the studies that have adopted the modified protocol of Viswanathan et al. (Kirkiewicz et al., 2016; Viswanathan et al., 2001). Moreover, a significant reduction in PhNR amplitude has been reported in glaucoma patients by Machida et al. (Bach and Poloschek, 2013; Machida et al., 2008). It is believed that the amplitude reduction is related to the severity of glaucoma (Machida, 2012).

Since PhNR is a slow broad wave, it makes it difficult not only to determine the peak amplitude but also the latency. Hence, PhNR latency is not commonly reported (Frishman et al., 2018; Lam, 2005). However, PhNR latency was significantly delayed in glaucoma patients compared to the control group in a study that used brief flashes stimuli (Viswanathan et al., 2001). Our findings, which showed low amplitude and longer latency,

thus agree with these previous results. To our knowledge, contradicting results have not been reported. The reason behind the similarity between our findings and the previous studies is the adoption of the modified protocol of PhNR recording that had been established by Viswanathan et al.

4.2.2. High sensitivity for PhNR amplitude

Calculating the sensitivity and specificity of a potential diagnostic test would determine the validity of adopting the test as a diagnostic tool (Parikh et al., 2008). PhNR effectiveness as a diagnostic test has been explored to determine its value in glaucoma detection (Viswanathan et al., 1999). With a long duration stimulus, PhNR amplitude had recorded sensitivity of 84% and a specificity of 94%, while with a short duration stimulus, the sensitivity and specificity were 95% and 91%, respectively (Viswanathan et al., 1999). The sensitivity and specificity based on the glaucoma stage have been explored in different studies. In the early stage of glaucoma, both sensitivity and specificity have been recorded with a range of 23.8-57 % and 90 - 92.3 %, respectively (Kirkiewicz et al., 2016; Machida et al., 2008, 2011). With moderate glaucoma, a sensitivity of 40.7 - 88.0 % and specificity of 97.4 % have been detected. These findings indicate that the PhNR can detect glaucomatous changes in moderate glaucoma better than early glaucoma. In the advanced stage of glaucoma, PhNR amplitude has shown its ability to detect glaucomatous changes based on a sensitivity and specificity that have been documented with a range of 66.7 - 93.0 % (Machida et al., 2008, 2011) and 92.3 - 97.4 %, respectively (Machida et al., 2011).

There is a consistency between our results and the study findings of Viswanathan et al. that used a long duration stimulus on non-human primates, in that we both recorded a high sensitivity for PhNR amplitude (Viswanathan et al., 1999). However, our recorded specificity for this test was lower (69.7%). To our knowledge, sensitivity and specificity of PhNR latency have not been reported in previous studies. However, in this thesis, we calculated the sensitivity and specificity for PhNR latency, and we determined a high specificity for the PhNR latency (96.7%). The reason behind the consistency between our findings and the Viswanathan et al. study is related to the same duration stimulus that has been used in our research protocol (Viswanathan et al., 1999). Due to our small sample size, further evaluation should be carried out to determine the sensitivity and specificity of PhNR latency with greater accuracy.

4.3. Significant mean deviation (MD) changes in glaucoma suspects and glaucoma groups

The aim of using SAP for glaucoma patients is to determine the presence and the severity of glaucoma. However, the initial test result might be inconclusive (Nouri-Mahdavi, 2014). It is believed that RGC loss due to glaucoma precedes the appearance of VF defects (Asaoka et al., 2014; Nouri-Mahdavi, 2014; Quigley et al., 1989). Furthermore, it has been reported that the structural changes related to glaucoma do not reflect the glaucomatous visual function changes (Kostianeva et al., 2016).

A significant difference in MD has been reported between glaucoma suspect and glaucoma patients in a study carried out by Asaoka et al. and Neoh et al. (Asaoka et al., 2014; Neoh et al., 1994). Their findings are consistent with our findings as we found a significant MD changes between glaucoma suspect and glaucoma groups. Although glaucoma progression can be diagnosed and monitored in many ways, adopting a reliable method to evaluate VF changes is crucial in glaucoma diagnosis (Cho et al., 2012; Nouri-Mahdavi, 2014; Odden et al., 2016).

4.4. Retinal nerve fiber layer (RNFL) thinning in both glaucoma suspect and glaucoma groups

Glaucoma changes in the form of irreversible RGC loss appear as reductions in the thickness of the RNFL (Sharma et al., 2008). The research that has been done by Schuman et al. and others has concluded that OCT had the ability to measure RNFL thickness (Bowd C et al., 2000; Schuman et al., 1995). Therefore, RNFL imaging assessment has been adopted for glaucoma diagnosis and management (Sharma et al., 2008). Also, it has been reported that OCT can identify early glaucomatous changes and might have the potential to diagnose and monitor glaucoma patients (Kanamori et al., 2003).

Our research finding reported a significant decrease in RNFL thickness in both glaucoma suspect and glaucoma groups which is consistent with the research that has been carried out by others (Kanamori et al., 2003; Parisi et al., 2001). It is also not clear if the

RNFL changes related to glaucoma represent the actual stage of the disease progression. Therefore, it is essential for clinicians to understand the limitations of OCT in terms of the possibility of artifacts and the floor effect, which is OCT's inability to detect RGCs when they are almost diminished (Dong et al., 2016; Leung et al., 2010). It is crucial for clinicians to base their decision not only on OCT results but also on other clinical evaluations.

5-Conclusion

Glaucoma is a silent disease, which makes it extremely challenging to find sensitive as well as specific clinical markers for early diagnosis (Weinreb et al., 2014; Wu et al., 2016). Therefore, determining the early glaucomatous changes is necessary to improve the management and the outcome of glaucoma patients. Adopting electrophysiological methods to evaluate the progressive loss of RGCs due to glaucoma can provide specific clinical markers (Wu et al., 2016). Exploring the possibility of using PERG and UF-ERG in the clinical setting has been evaluated on both humans and non-human primates, and these studies showed promising results (Bach et al., 2013; Kreuz et al., 2014; Ventura et al., 2013). Moreover, using UF-ERG in the clinical setting has shown its potential to be used in glaucoma diagnosis. Overall, the work done in this thesis showed that PERG checks and bars showed a similar ability to detect individuals without glaucomatous changes. In addition, PhNR amplitude and latency showed the ability to identify individuals with or without glaucomatous changes.

References

Asaoka, R., Iwase, A., Hirasawa, K., Murata, H., and Araie, M. (2014). Identifying "preperimetric" glaucoma in standard automated perimetry visual fields. Invest. Ophthalmol. Vis. Sci. *55*, 7814–7820.

Bach, M., and Hoffmann, M.B. (2008). Update on the pattern electroretinogram in glaucoma. Optom. Vis. Sci. Off. Publ. Am. Acad. Optom. *85*, 386–395.

Bach, M., and Poloschek, C.M. (2013). Electrophysiology and glaucoma: current status and future challenges. Cell Tissue Res. *353*, 287–296.

Bach, M., Hiss, P., and Röver, J. (1988). Check-size specific changes of pattern electroretinogram in patients with early open-angle glaucoma. Doc. Ophthalmol. Adv. Ophthalmol. *69*, 315–322.

Bach, M., Hawlina, M., Holder, G., Marmor, M., Meigen, T., Vaegan, Y., and Miyake, Y. (2000). Standard for pattern electroretinography. Doc. Ophthalmol. *101*, 11–18.

Bach, M., Unsoeld, A.S., Philippin, H., Staubach, F., Maier, P., Walter, H.S., Bomer, T.G., and Funk, J. (2006). Pattern ERG as an early glaucoma indicator in ocular hypertension: a long-term, prospective study. Invest. Ophthalmol. Vis. Sci. *47*, 4881.

Bach, M., Brigell, M., Hawlina, M., Holder, G., Johnson, M., McCulloch, D., Meigen, T., and Viswanathan, S. (2013). ISCEV standard for clinical pattern electroretinography (PERG): 2012 update. J. Clin. Electrophysiol. Vis. - Off. J. Int. Soc. Clin. Electrophysiol. Vis. *126*, 1–7.

Banitt, M.R., Ventura, L.M., Feuer, W.J., Savatovsky, E., Luna, G., Shif, O., Bosse, B., and Porciatti, V. (2013). Progressive loss of retinal ganglion cell function precedes structural loss by several years in glaucoma suspects. Invest. Ophthalmol. Vis. Sci. *54*, 2346.

Bearse, M.A., Adams, A.J., Han, Y., Schneck, M.E., Ng, J., Bronson-Castain, K., and Barez, S. (2006). A multifocal electroretinogram model predicting the development of diabetic retinopathy. Prog. Retin. Eye Res. *25*, 425–448.

van den Berg, T.J., Riemslag, F.C., de Vos, G.W., and Verduyn Lunel, H.F. (1986). Pattern ERG and glaucomatous visual field defects. Doc. Ophthalmol. Adv. Ophthalmol. *61*, 335–341.

Berninger, T., and Schuurmans, R.P. (1985). Spatial tuning of the pattern ERG across temporal frequency. Doc. Ophthalmol. Adv. Ophthalmol. *61*, 17–25.

Birch DG, and Anderson JL (1992). Standardized full-field electroretinography: Normal values and their variation with age. Arch. Ophthalmol. *110*, 1571–1576.

Bode, S.F.N., Jehle, T., and Bach, M. (2011). Pattern Electroretinogram in Glaucoma Suspects: New Findings from a Longitudinal Study. Invest. Ophthalmol. Vis. Sci. *52*, 4300–4306.

Bowd, C., Tafreshi, A., Vizzeri, G., Zangwill, L.M., Sample, P.A., and Weinreb, R.N. (2009a). Repeatability of pattern electroretinogram measurements using a new paradigm optimized for glaucoma detection. J. Glaucoma *18*, 437–442.

Bowd, C., Vizzeri, G., Tafreshi, A., Zangwill, L.M., Sample, P.A., and Weinreb, R.N. (2009b). Diagnostic Accuracy of Pattern Electroretinogram Optimized for Glaucoma Detection. Ophthalmology *116*, 437–443.

Bowd, C., Tafreshi, A., Zangwill, L.M., Medeiros, F.A., Sample, P.A., and Weinreb, R.N. (2011). Pattern electroretinogram association with spectral domain-OCT structural measurements in glaucoma. Eye *25*, 224–232.

Bowd C, Weinreb RN, Williams JM, and Zangwill LM (2000). The retinal nerve fiber layer thickness in ocular hypertensive, normal, and glaucomatous eyes with optical coherence tomography. Arch. Ophthalmol. *118*, 22–26.

Brown, K.T., and Watanabe, K. (1962). Isolation and identification of a receptor potential from the pure cone fovea of the monkey retina. Nature *193*, 958 passim.

Carpi, F., and Tomei, F. (2006). Non-invasive electroretinography. Biomed. Pharmacother. *60*, 375–379.

Cassin, B. (1995). Fundamentals for ophthalmic technical personnel (Philadelphia : Saunders).

Celesia, G.G., Kaufman, D., and Cone, S. (1987). Effects of age and sex on pattern electroretinograms and visual evoked potentials. Electroencephalogr. Clin. Neurophysiol. *68*, 161–171.

Cho, J., Sung, K., Yun, S.-C., Na, J., Lee, Y., and Kook, M. (2012). Progression detection in different stages of glaucoma: mean deviation versus visual field index. Jpn. J. Ophthalmol. *56*, 128–133.

la Cour, M., and Ehinger, B. (2005). The Retina. In Advances in Organ Biology, J. Fischbarg, ed. (Elsevier), pp. 195–252.

Cvenkel, B., Sustar, M., and Perovšek, D. (2017). Ganglion cell loss in early glaucoma, as assessed by photopic negative response, pattern electroretinogram, and spectral-domain optical coherence tomography. Doc. Ophthalmol. *135*, 17–28.

Davis, B., Crawley, L., Pahlitzsch, M., Javaid, F., and Cordeiro, M. (2016). Glaucoma: the retina and beyond. Acta Neuropathol. (Berl.) *132*, 807–826.

Denniston, A.K.., and Murray, P.I. (2006). Oxford handbook of ophthalmology (oxford university press inc).

Distelhorst, J.S., and Hughes, G.M. (2003). Open-angle glaucoma. Am. Fam. Physician *67*, 1937–1944.

Dong, Z.M., Wollstein, G., and Schuman, J.S. (2016). Clinical Utility of Optical Coherence Tomography in Glaucoma. Invest. Ophthalmol. Vis. Sci. *57*, OCT556.

Evers, H.U., and Gouras, P. (1986). Three cone mechanisms in the primate electroretinogram: two with, one without off-center bipolar responses. Vision Res. *26*, 245–254.

Fiorentini, A., Maffei, L., Pirchio, M., Spinelli, D., and Porciatti, V. (1981). The ERG in response to alternating gratings in patients with diseases of the peripheral visual pathway. Invest. Ophthalmol. Vis. Sci. *21*, 490–493.

Fishman, G.A. (1985). Basic principles of clinical electroretinography. Retina Phila. Pa *5*, 123–126.

Fredette, M.-J., Anderson, D.R., Porciatti, V., and Feuer, W. (2008). Reproducibility of pattern electroretinogram in glaucoma patients with a range of severity of disease with the new glaucoma paradigm. Ophthalmology *115*, 957–963.

Frishman, L., Sustar, M., Kremers, J., McAnany, J.J., Sarossy, M., Tzekov, R., and Viswanathan, S. (2018). ISCEV extended protocol for the photopic negative response (PhNR) of the full-field electroretinogram. Doc. Ophthalmol. *136*, 207–211.

Frishman, L.J., Shen, F.F., Du, L., Robson, J.G., Harwerth, R.S., Smith, E.L., Carter-Dawson, L., and Crawford, M.L. (1996). The scotopic electroretinogram of macaque after retinal ganglion cell loss from experimental glaucoma. Invest. Ophthalmol. Vis. Sci. *37*, 125–141.

Ganekal, S., Dorairaj, S., and Jhanji, V. (2013). Pattern Electroretinography Changes in Patients with Established or Suspected Primary Open Angle Glaucoma. J. Curr. Glaucoma Pract. *7*, 39–42.

Glovinsky, Y., Quigley, H.A., and Dunkelberger, G.R. (1991). Retinal ganglion cell loss is size dependent in experimental glaucoma. Invest. Ophthalmol. Vis. Sci. *32*, 484–491.

Graham, S.L., Drance, S.M., Chauhan, B.C., Swindale, N.V., Hnik, P., Mikelberg, F.S., and Douglas, G.R. (1996). Comparison of psychophysical and electrophysiological testing in early glaucoma. Invest. Ophthalmol. Vis. Sci. *37*, 2651–2662.

Harwerth, R.S., Smith, E.L., and DeSantis, L. (1997). Experimental glaucoma: perimetric field defects and intraocular pressure. J. Glaucoma *6*, 390–401.

Harwerth, R.S., Wheat, J.L., Fredette, M.J., and Anderson, D.R. (2010). Linking structure and function in glaucoma. Prog. Retin. Eye Res. *29*, 249–271.

Heckenlively, J.R., and Arden, G.B. (Geoffrey B. (2006). Principles and practice of clinical electrophysiology of vision (Cambridge, Mass.: Cambridge, Mass. : MIT Press, c2006.).

Heijl, A., and Patella, V.M. (2002). Essential perimetry: The field analyzer primer (Dublin, Calif.: Carl Zeiss Meditec, Inc.).

Heynen, H., and van Norren, D. (1985). Origin of the electroretinogram in the intact macaque eye--II. Current source-density analysis. Vision Res. *25*, 709–715.

Hiss, P., and Fahl, G. (1991). [Changes in the pattern electroretinogram in glaucoma and ocular hypertension are dependent on stimulus frequency]. Fortschritte Ophthalmol. Z. Dtsch. Ophthalmol. Ges. *88*, 562–565.

Holder, G.E. (1987). Significance of abnormal pattern electroretinography in anterior visual pathway dysfunction. Br. J. Ophthalmol. *71*, 166–171.

Holder, G.E. (2001). Pattern electroretinography (PERG) and an integrated approach to visual pathway diagnosis. Prog. Retin. Eye Res. *20*, 531–561.

Hood, D.C., Xu, L., Thienprasiddhi, P., Odel, J.G., Grippo, T.M., Liebmann, J.M., Ritch, R., and Greenstein, V.C. (2005). The pattern electroretinogram in glaucoma patients with confirmed visual field deficits. Invest. Ophthalmol. Vis. Sci. *46*, 2411–2418.

Jafarzadehpour, E., Radinmehr, F., Pakravan, M., Mirzajani, A., and Yazdani, S. (2013). Pattern Electroretinography in Glaucoma Suspects and Early Primary Open Angle Glaucoma. J. Ophthalmic Vis. Res. *8*, 199–206.

Jampol, L.M. (2001). Electrophysiologic Testing in Disorders of the Retina, Optic Nerve, and Visual Pathway, 2nd edition,: by Gerald A. Fishman, David G. Birch, Graham E. Holder, and Mitchell G. Brigell, San Francisco, Foundation of the American Academy of Ophthalmology, Ophthalmology Monographs #2, 2001, 308 pp, illus. Surv. Ophthalmol. *46*, 302–303.

Johnson, M.A., Drum, B.A., Quigley, H.A., Sanchez, R.M., and Dunkelberger, G.R. (1989). Pattern-evoked potentials and optic nerve fiber loss in monocular laser-induced glaucoma. Invest. Ophthalmol. Vis. Sci. *30*, 897–907.

Jonas, J.B., Aung, T., Bourne, R.R., Bron, A.M., Ritch, R., and Panda-Jonas, S. (2017). Glaucoma. The Lancet.

Kanamori, A., Nakamura, M., Escano, M.F.., Seya, R., Maeda, H., and Negi, A. (2003). Evaluation of the glaucomatous damage on retinal nerve fiber layer thickness measured by optical coherence tomography. Am. J. Ophthalmol. *135*, 513–520.

King, A., Azuara-Blanco, A., and Tuulonen, A. (2013). Glaucoma. BMJ *346*.

Kinoshita, J., Takada, S., Iwata, N., and Tani, Y. (2016). Comparison of photopic negative response (PhNR) between focal macular and full-field electroretinograms in monkeys. Doc. Ophthalmol. *132*, 177–187.

Kirkiewicz, M., Lubiński, W., and Penkala, K. (2016). Photopic negative response of full-field electroretinography in patients with different stages of glaucomatous optic neuropathy. J. Clin. Electrophysiol. Vis. - Off. J. Int. Soc. Clin. Electrophysiol. Vis. *132*, 57–65.

Korth, M. (1997). The value of electrophysiological testing in glaucomatous diseases. J. Glaucoma *6*, 331–343.

Korth, M., Horn, F., and Jonas, J. (1993). Utility of the color pattern-electroretinogram (PERG) in glaucoma. Graefes Arch. Clin. Exp. Ophthalmol. Albrecht Von Graefes Arch. Klin. Exp. Ophthalmol. *231*, 84.

Kostianeva, S.S., Konareva-Kostianeva, M.I., and Atanassov, M.A. (2016). Relationship between visual field changes and optical coherence tomography measurements in advanced open-angle glaucoma. Folia Med. (Plovdiv) *58*, 174–181.

Kreuz, A.C., Oyamada, M.K., Hatanaka, M., and Monteiro, M.L.R. (2014). The role of pattern-reversal electroretinography in the diagnosis of glaucoma. Arq. Bras. Oftalmol. *77*, 403–410.

Kundra, H., Park, J.C., and McAnany, J.J. (2016). Comparison of photopic negative response measurements in the time and time-frequency domains. Doc. Ophthalmol. Adv. Ophthalmol. *133*, 91–98.

Lam, B.L. (2005). Electrophysiology of vision clinical testing and applications (Boca Raton: Boca Raton : Taylor & Francis, 2005.).

Leung, K.-S., Christopher (2014). Diagnosing glaucoma progression with optical coherence tomography. Curr. Opin. Ophthalmol. *25*, 104–111.

Leung, C.K., Cheung, C.Y.L., Weinreb, R.N., Qiu, K., Liu, S., Li, H., Xu, G., Fan, N., Pang, C.P., Tse, K.K., et al. (2010). Evaluation of retinal nerve fiber layer progression in glaucoma: a study on optical coherence tomography guided progression analysis. Invest. Ophthalmol. Vis. Sci. *51*, 217–222.

Luo, X., and Frishman, L.J. (2011). Retinal pathway origins of the pattern electroretinogram (PERG). Invest. Ophthalmol. Vis. Sci. *52*, 8571.

M. Bach (2001). Electrophysiological Approaches for Early Detection of Glaucoma. Eur. J. Ophthalmol. *11*, 41–49.

Machida, S. (2012). Clinical applications of the photopic negative response to optic nerve and retinal diseases. J. Ophthalmol. *2012*, 397178.

Machida, S., Gotoh, Y., Toba, Y., Ohtaki, A., Kaneko, M., and Kurosaka, D. (2008). Correlation between photopic negative response and retinal nerve fiber layer thickness and optic disc topography in glaucomatous eyes. Invest. Ophthalmol. Vis. Sci. *49*, 2201–2207.

Machida, S., Tamada, K., Oikawa, T., Gotoh, Y., Nishimura, T., Kaneko, M., and Kurosaka, D. (2011). Comparison of photopic negative response of full-field and focal electroretinograms in detecting glaucomatous eyes. J. Ophthalmol. *2011*.

Mafei, L., and Fiorentini, A. (1981). Electroretinographic responses to alternating gratings before and after section of the optic nerve. Science *211*, 953–955.

Mantravadi, A.V., and Vadhar, N. (2015). Glaucoma. Prim. Care Ophthalmol. *42*, 437–449.

Marmor, M.F., and Zrenner, E. (1998). Standard for clinical electroretinography (1999 update). International Society for Clinical Electrophysiology of Vision. Doc. Ophthalmol. Adv. Ophthalmol. *97*, 143–156.

Marx, M.S., Podos, S.M., Bodis-Wollner, I., Howard-Williams, J.R., Siegel, M.J., Teitelbaum, C.S., Maclin, E.L., and Severin, C. (1986). Flash and pattern electroretinograms in normal and laser-induced glaucomatous primate eyes. Invest. Ophthalmol. Vis. Sci. *27*, 378–386.

Mavilio, A., Scrimieri, F., and Errico, D. (2015). Can Variability of Pattern ERG Signal Help to Detect Retinal Ganglion Cells Dysfunction in Glaucomatous Eyes BioMed Res. Int. *2015*, 571314.

May, J.G., Ralston, J.V., Reed, J.L., and Van Dyk, H.J.L. (1982). Loss in Pattern-Elicited Electroretinograms in Optic Nerve Dysfunction. Am. J. Ophthalmol. *93*, 418–422.

Mescher, A.L. (2016). The Eye & Ear: Special Sense Organs. In Junqueira's Basic Histology, 14e, (New York, NY: McGraw-Hill Education), p.

Michelessi, M., Lucenteforte, E., Oddone, F., Brazzelli, M., Parravano, M., Franchi, S., Ng, S.M., and Virgili, G. (2015). Optic nerve head and fibre layer imaging for diagnosing glaucoma. Cochrane Database Syst. Rev. CD008803.

Miglior, S., Brigatti, L., Lonati, C., Rossetti, L., Pierrottet, C., and Orzalesi, N. (1996). Correlation between the progression of optic disc and visual field changes in glaucoma. Curr. Eye Res. *15*, 145–149.

Miura, G., Wang, M.H., Ivers, K.M., and Frishman, L.J. (2009). Retinal pathway origins of the pattern ERG of the mouse. Exp. Eye Res. *89*, 49–62.

Neoh, C., Kaye, S.B., Brown, M., Ansons, A.M., and Wishart, P. (1994). Pattern electroretinogram and automated perimetry in patients with glaucoma and ocular hypertension. Br. J. Ophthalmol. *78*, 359–362.

Nickells, R.W. (2012). The Cell and Molecular Biology of Glaucoma: Mechanisms of Retinal Ganglion Cell Death. Invest. Ophthalmol. Vis. Sci. *53*, 2476–2481.

Nouri-Mahdavi, K. (2014). Selecting visual field tests and assessing visual field deterioration in glaucoma. Can. J. Ophthalmol. Can. Ophtalmol. *49*, 497–505.

Odden, J.L., Mihailovic, A., Boland, M.V., Friedman, D.S., West, S.K., and Ramulu, P.Y. (2016). Evaluation of Central and Peripheral Visual Field Concordance in Glaucoma. Invest. Ophthalmol. Vis. Sci. *57*, 2797–2804.

Oddone, F., Lucenteforte, E., Michelessi, M., Rizzo, S., Donati, S., Parravano, M., and Virgili, G. (2016). Macular versus Retinal Nerve Fiber Layer Parameters for Diagnosing Manifest Glaucoma: A Systematic Review of Diagnostic Accuracy Studies. Ophthalmology *123*, 939–949.

O'Donaghue, E., Arden, G.B., O'Sullivan, F., Falcão-Reis, F., Moriarty, B., Hitchings, R.A., Spilleers, W., Hogg, C., and Weinstein, G. (1992). The pattern electroretinogram in glaucoma and ocular hypertension. Br. J. Ophthalmol. *76*, 387–394.

Papst, N., Bopp, M., and Schnaudigel, O.E. (1984). The pattern evoked electroretinogram associated with elevated intraocular pressure. Graefes Arch. Clin. Exp. Ophthalmol. Albrecht Von Graefes Arch. Klin. Exp. Ophthalmol. *222*, 34–37.

Parikh, R., Mathai, A., Parikh, S., Chandra Sekhar, G., and Thomas, R. (2008). Understanding and using sensitivity, specificity and predictive values. Indian J. Ophthalmol. *56*, 45–50.

Parisi, V., Manni, G., Centofanti, M., Gandolfi, S.A., Olzi, D., and Bucci, M.G. (2001). Correlation between optical coherence tomography, pattern electroretinogram, and visual evoked potentials in open-angle glaucoma patients. Ophthalmology *108*, 905–912.

Patel, K., and Patel, S. (2014). Angle-closure glaucoma. Clin. Top. Ophthalmol. *60*, 254–262.

Pfeiffer, N., and Bach, M. (1992). The pattern-electroretinogram in glaucoma and ocular hypertension. A cross-sectional and longitudinal study. Ger. J. Ophthalmol. *1*, 35–40.

Podoleanu, A.G. (2012). Optical coherence tomography. J. Microsc. *247*, 209–219.

Porciatti, V. (2015). Electrophysiological assessment of retinal ganglion cell function. Exp. Eye Res. *141*, 164–170.

Porciatti, V., and Ventura, L.M. (2004). Normative data for a user-friendly paradigm for pattern electroretinogram recording. Ophthalmology *111*, 161–168.

Porciatti, V., Falsini, B., Brunori, S., Colotto, A., and Moretti, G. (1987). Pattern electroretinogram as a function of spatial frequency in ocular hypertension and early glaucoma. Doc. Ophthalmol. Adv. Ophthalmol. *65*, 349–355.

Preiser, D., Lagrèze, W.A., Bach, M., and Poloschek, C.M. (2013). Photopic negative response versus pattern electroretinogram in early glaucoma. Invest. Ophthalmol. Vis. Sci. *54*, 1182.

Quigley, H.A. (2011). Glaucoma. The Lancet *377*, 1367–1377.

Quigley, H.A., Dunkelberger, G.R., and Green, W.R. (1989). Retinal ganglion cell atrophy correlated with automated perimetry in human eyes with glaucoma. Am. J. Ophthalmol. *107*, 453–464.

Rafuse, P.E., and Buys, Y.M. (2009). Canadian Ophthalmological Society evidence-based clinical practice guidelines for the management of glaucoma in the adult eye. Can. J. Ophthalmol. J. Can. Ophtalmol. *44 suppl 1*, S7–93.

Randall, T., and Melton, R. (2004). Risk Factors for Glaucoma. Rev. Optom. 4–6.

Rangaswamy, N.V., Frishman, L.J., Dorotheo, E.U., Schiffman, J.S., Bahrani, H.M., and Tang, R.A. (2004). Photopic ERGs in patients with optic neuropathies: comparison with primate ERGs after pharmacologic blockade of inner retina. Invest. Ophthalmol. Vis. Sci. *45*, 3827–3837.

Remington, L.A. (2012). Chapter 4 - Retina. In Clinical Anatomy and Physiology of the Visual System (Third Edition), (Saint Louis: Butterworth-Heinemann), pp. 61–92.

Ringens, P.J., Vijfvinkel-Bruinenga, S., and van Lith, G.H. (1986). The pattern-elicited electroretinogram. I. A tool in the early detection of glaucoma? Ophthalmol. J. Int. Ophtalmol. Int. J. Ophthalmol. Z. Augenheilkd. *192*, 171–175.

Roy, M.S., Barsoum-Homsy, M., Hanna, N., Chevrette, L., and Trick, G.L. (1997). Pattern electroretinogram and spatial contrast sensitivity in primary congenital glaucoma. Ophthalmology *104*, 2136–2142.

Schuman, J.S., Hee, M.R., Puliafito, C.A., Wong, C., Pedut-Kloizman, T., Lin, C.P., Hertzmark, E., Izatt, J.A., Swanson, E.A., and Fujimoto, J.G. (1995). Quantification of Nerve Fiber Layer Thickness in Normal and Glaucomatous Eyes Using Optical Coherence Tomography: A Pilot Study. Arch. Ophthalmol. *113*, 586–596.

Schuman, J.S., Puliafito, C.A., and Fujimoto, J.G. (2004). optical coherence tomography of ocular disease (Slack incorporated).

Schuurmans, R.P., and Berninger, T. (1985). Luminance and contrast responses recorded in man and cat. Doc. Ophthalmol. Adv. Ophthalmol. *59*, 187–197.

Sehi, J., Mitra, Pinzon-Plazas, S., Mariana, Feuer, S., William, and Greenfield, S., David (2009). Relationship Between Pattern Electroretinogram, Standard Automated Perimetry, and Optic Nerve Structural Assessments. J. Glaucoma *18*, 608–617.

Sehi, M., Grewal, D.S., Goodkin, M.L., and Greenfield, D.S. (2010). Reversal of Retinal Ganglion Cell Dysfunction after Surgical Reduction of Intraocular Pressure. Ophthalmology *117*, 2329–2336.

Sharma, P., Sample, P.A., Zangwill, L.M., and Schuman, J.S. (2008). Diagnostic Tools for Glaucoma Detection and Management. Surv. Ophthalmol. *53*, S17–S32.

Sieving, P.A., Frishman, L.J., and Steinberg, R.H. (1986). Scotopic threshold response of proximal retina in cat. J. Neurophysiol. *56*, 1049–1061.

Sieving, P.A., Murayama, K., and Naarendorp, F. (1994). Push-pull model of the primate photopic electroretinogram: a role for hyperpolarizing neurons in shaping the b-wave. Vis. Neurosci. *11*, 519–532.

Skalicky, S.E. (2016). Visual Electrophysiology. In Ocular and Visual Physiology, (Springer, Singapore), pp. 155–166.

Smith, C.A., Vianna, J.R., and Chauhan, B.C. (2017). Assessing retinal ganglion cell damage. Eye Lond. Engl. *31*, 209–217.

Tortora, G.J. (2012). Principles of human anatomy (Hoboken, NJ: Hoboken, NJ : John Wiley, c2012.).

Trick, G.L. (1985). Retinal potentials in patients with primary open-angle glaucoma: physiological evidence for temporal frequency tuning deficits. Invest. Ophthalmol. Vis. Sci. *26*, 1750–1758.

Trick, L., Gary (1992). Pattern Electroretinogram: An Electrophysiological Technique Applicable to Primary Open-Angle Glaucoma and Ocular Hypertension. J. Glaucoma *1*, 271–279.

Varma, R., Quigley, H.A., and Pease, M.E. (1992). Changes in optic disk characteristics and number of nerve fibers in experimental glaucoma. Am. J. Ophthalmol. *114*, 554–559.

Ventura, L.M., Porciatti, V., Ishida, K., Feuer, W.J., and Parrish, R.K. (2005). Pattern electroretinogram abnormality and glaucoma. Ophthalmology *112*, 10–19.

Ventura, L.M., Golubev, I., Feuer, W.J., and Porciatti, V. (2013). Pattern electroretinogram progression in glaucoma suspects. J. Glaucoma *22*, 219.

Viswanathan, S., Frishman, L.J., Robson, J.G., Harwerth, R.S., and Smith, E.L. (1999). The photopic negative response of the macaque electroretinogram: reduction by experimental glaucoma. Invest. Ophthalmol. Vis. Sci. *40*, 1124–1136.

Viswanathan, S., Frishman, L.J., and Robson, J.G. (2000). The uniform field and pattern ERG in macaques with experimental glaucoma: removal of spiking activity. Invest. Ophthalmol. Vis. Sci. *41*, 2797–2810.

Viswanathan, S., Frishman, L.J., Robson, J.G., and Walters, J.W. (2001). The Photopic Negative Response of the Flash Electroretinogram in Primary Open Angle Glaucoma. Invest. Ophthalmol. Vis. Sci. *42*, 514–522.

Von Thun Und Hohenstein-Blaul, N., Kunst, S., Pfeiffer, N., and Grus, F.H. (2017). Biomarkers for glaucoma: from the lab to the clinic. Eye Lond. Engl. *31*, 225–231.

Wachtmeister, L. (1998). Oscillatory potentials in the retina: what do they reveal. Prog. Retin. Eye Res. *17*, 485–521.

Wanger, P., and Persson, H.E. (1983). Pattern-reversal electroretinograms in unilateral glaucoma. Invest. Ophthalmol. Vis. Sci. *24*, 749.

Weinreb, R.N., Aung, T., and Medeiros, F.A. (2014). The Pathophysiology and Treatment of Glaucoma: A Review. *311*, 1901–1911.

Whitten, D.N., and Brown, K.T. (1973). The time courses of late receptor potentials from monkey cones and rods. Vision Res. *13*, 107–135.

Wilsey, L.J., and Fortune, B. (2016). Electroretinography in glaucoma diagnosis. Curr. Opin. Ophthalmol. *27*, 118–124.

Wolfgang, D., and Fujimoto, J.G. (2015). Optical coherence tomography : technology and applications (Cham : SpringerReference, 2015.).

Yang, A., and Swanson, W.H. (2007). A new pattern electroretinogram paradigm evaluated in terms of user friendliness and agreement with perimetry. Ophthalmology *114*, 671–679.

Yaqub, M. (2012). Visual fields interpretation in glaucoma: a focus on static automated perimetry. Community Eye Health *25*, 1–8.